Geoscience Frontiers 13 (2022) 101402

Contents lists available at ScienceDirect

Geoscience Frontiers

journal homepage: www.elsevier.com/locate/gsf

Research Paper

The generation and evolution of the Archean continental crust: The granitoid story in southeastern Brazil

Rodrigo S. Marimon [a,*], Chris J. Hawkesworth [b], Elton L. Dantas [c], Rudolph A.J. Trouw [a], Wilson Teixeira [d], Peter C. Hackspacher [e,†], Allen Fetter [e], Ciro A. Ávila [a], Silvia Volante [f,g], Atlas V. Corrêa Neto [a], Everton M. Bongiolo [h], Rodrigo Vinagre [a], Maurício Simon [a]

[a] Depto. de Geologia, IGEO, Universidade Federal do Rio de Janeiro, UFRJ, Rio de Janeiro, RJ, Brazil
[b] School of Earth Sciences, University of Bristol, Bristol, United Kingdom
[c] Instituto de Geociências, Universidade de Brasília, UnB, Brasília, DF, Brazil
[d] Instituto de Geociências, Universidade de São Paulo, USP, São Paulo, SP, Brazil
[e] Instituto de Geociências e Ciências Exatas, Universidade Estadual Paulista, Rio Claro, SP, Brazil
[f] Institute of Geology, Mineralogy and Geophysics, Ruhr-Universität Bochum, Universitätsstraße 150, 44801 Bochum, Germany
[g] ISOTOPIA Lab, School of Earth, Atmosphere and Environment, Monash University, Wellington Rd, Clayton, VIC 3800, Australia
[h] Programa de Pós-Graduação em Geociências, IG, Universidade Federal do Rio Grande do Sul, UFRGS, Porto Alegre, RS, Brazil

ARTICLE INFO

Article history:
Received 11 January 2022
Revised 14 April 2022
Accepted 5 May 2022
Available online 06 May 2022
Handling Editor: M. Santosh

Keywords:
Granitoid petrogenesis
Archean geodynamics
Crustal evolution
TTGs
A-types
Batch melting calculations

ABSTRACT

The Archean Eon was a time of geodynamic changes. Direct evidence of these transitions come from igneous/metaigneous rocks, which dominate cratonic segments worldwide. New data for granitoids from an Archean basement inlier related to the Southern São Francisco Craton (SSFC), are integrated with geochronological, isotopic and geochemical data on Archean granitoids from the SSFC. The rocks are divided into three main geochemical groups with different ages: (1) TTG (3.02–2.77 Ga); (2) medium- to high-K granitoids (2.85–2.72 Ga); and (3) A-type granites (2.7–2.6 Ga). The juvenile to chondritic (Hf-Nd isotopes) TTG were divided into two sub-groups, TTG 1 (low-HREE) and 2 (high-HREE), derived from partial melting of metamafic rocks similar to those from adjacent greenstone belts. The compositional diversity within the TTG is attributed to different pressures during partial melting, supported by a positive correlation of Dy/Yb and Sr/Zr, and batch melting calculations. The proposed TTG sources are geochemically similar to basaltic rocks from modern island-arcs, indicating the presence of subduction processes concomitant with TTG emplacement. From ~2.85 Ga to 2.70 Ga, the dominant rocks were K-rich granitoids. These are modeled as crustal melts of TTG, during regional metamorphism indicative of crustal thickening. Their compositional diversity is linked to: (i) differences in source composition; (ii) distinct melt fractions during partial melting; and (iii) different residual mineralogies reflecting varying P–T conditions. Post-collisional (~2.7–2.6 Ga) A-type granites reflect rifting in that they were closely followed by extension-related dyke swarms, and they are interpreted as differentiation or partial melting products of magmas derived from subduction-modified mantle. The sequence of granitoid emplacement indicates subduction-related magmatism was followed by crustal thickening, regional metamorphism and crustal melting, and post-collisional extension, similar to that seen in younger Wilson Cycles. It is compelling evidence that plate tectonics was active in this segment of Brazil from ~3 Ga.

1. Introduction

The Archean Eon remains one of the most critical periods of the Earth's history. The 3.2–2.8 Ga time interval is often regarded as the transition from stagnant lid geodynamics towards modern-style-like plate tectonics, characterized by large-scale cyclic assembly and break-up of landmasses (e.g., Laurent et al., 2014a; Dhuime et al., 2015; Smit and Mezger, 2017; Holder et al., 2019; Brown et al., 2020; Hawkesworth et al., 2020). Although discrete, localized events of subduction (or dripduction) and collision may have occurred before 3.2–2.8 Ga, plate tectonics may not have been

* Corresponding author.
E-mail address: rsmarimon@ufrj.br (R.S. Marimon).
† Deceased.

https://doi.org/10.1016/j.gsf.2022.101402
1674-9871/

the dominant dynamic mode until the late Archaean (e.g., Hawkesworth et al., 2020).

TTG are the most voluminous constituents of Archean cratons worldwide (e.g., Laurent et al., 2014a) and so they have attracted a lot of attention from researchers investigating the geodynamics of Archean settings (e.g., Moyen and Martin, 2012 and references therein). TTG are geochemically diverse, and this has been attributed to: (i) variations in pressure during partial melting of mafic lithologies (e.g., Moyen, 2011; Palin et al., 2016); (ii) differences in the content of free water in the mafic source during partial melting (e.g., Pourteau et al., 2020); and (iii) fractionation and/or solid–liquid unmixing involving plagioclase and amphibole (e.g., Laurent et al., 2020). It is likely that each of these processes occurred in different regions at different periods during the evolution of the Archean Earth. TTG from the Southern Brasília Orogen and the Southern São Francisco Craton are also geochemically diverse (e.g., Farina et al., 2015; Cioffi et al., 2016a, 2016b) and, in this contribution, we use geochemistry to verify which of the proposed models best explain the characteristics of the analyzed TTG. Batch melting calculations of mafic rocks from regional greenstone belts constrain the geodynamic and petrogenetic scenarios for the generation of the TTG.

In many cratons the Meso-Neoarchean transition is marked by a shift from sodic (TTG-dominated) to potassic magmatism (Laurent et al., 2014a and references therein). Two groups of medium- to high-K suites are recognized: K-rich granites interpreted as partial melts of crustal lithologies, and sanukitoids and certain A-types granites thought to represent differentiation products of partial melting of incompatible-element-rich mantle, which may in some cases reflect previous subduction processes (Shirey and Hanson, 1984; Martin et al., 2009; Heilimo et al., 2010; Laurent et al., 2011, 2013, 2014a and references therein). Sanukitoids bear some similarities to basalt-andesite-dacite-rhyolite suites (BADR), which dominate modern subduction settings (e.g., Martin et al., 2009), but differences also standout such as stronger HREE fractionation and higher contents of Ba, Sr and K_2O in the sanukitoids *sensu stricto* (e.g., Heilimo et al., 2010). Batch melting calculations, supported by partial melting experiments, are used to investigate the petrogenesis of medium- to high-K granites from the Southern Brasília Orogen and São Francisco Craton and, for instance, whether the partial melting of TTG at different P-T conditions can explain the observed compositional diversity of Archean granites in the considered regions. A-type high-K rocks are recognized and they provide new constraints on models of late-stage lithospheric extension.

The Archean geodynamics have long been an issue of intense debate, especially whether plate tectonics operated in the early Archean (i.e., prior to 3.0 Ga). Some suggest that plate tectonics has been dominant on Earth since the early Hadean (e.g., Kusky et al., 2021; Windley et al., 2021, among others); whereas others invoke a regime transition at ~3.2–2.8 Ga, when plate tectonics became dominant at a global scale following a period of stagnant or squishy-lid regime (e.g., Moyen and Martin, 2012; Laurent et al., 2014a; Bédard, 2018; Hawkesworth et al., 2020, among others). The nature of geodynamic and geotectonic shifts is imprinted upon the most voluminous constituents of the continental crust: its metaigneous rocks. We investigate whether the sequence of granitoid emplacement in the Southern Brasília Orogen and Southern São Francisco Craton is consistent with plate tectonics since ~3.0 Ga and whether primitive mafic lithologies from greenstone belts of the Southern São Francisco Craton (e.g., Brando-Soares et al., 2020), portions of which are older than 2.95 Ga, bear similarities with rocks produced in modern subduction-related tectonic environments.

In summary, we present new geochemical, isotopic and geochronological data on granitoids from a Meso- to Neo-archean basement inlier in the Southern Brasília Orogen, southeastern Brazil, and integrate the data with available results from the adjacent Southern São Francisco Craton. The compositional evolution of mafic and felsic rocks is integrated with a large dataset of experimental melts, and batch melting calculations, to constrain the conditions of magma generation and their relation to different geodynamic settings from 3.1 Ga to 2.6 Ga.

2. Geological background

2.1. Archean nuclei of the São Francisco Craton

The São Francisco Craton is one of the largest and best exposed shield areas in South America. The southern segment of the craton consists of a series of Archean nuclei with a history of accretionary/collisional processes (mostly from 3.00 to 2.75 Ga) that culminated in the amalgamation of a number of terrains (e.g., Albert et al., 2016). Archean rocks and collisional fabrics were remobilized during renewed accretion followed by continental collision in the Paleoproterozoic (2.1–2.0 Ga suture zones), which is taken to mark the timing of paleocontinent stabilization (Alkmim and Marshak, 1998; Noce et al., 2007; Ávila et al., 2010, 2014; Barbosa et al., 2015; Teixeira et al., 2015, 2017; Aguilar et al., 2017). The São Francisco Craton is the foreland of Neoproterozoic fold belt systems (Brasiliano/Pan-African event) and it has remained virtually unaffected since Paleoproterozoic times (Teixeira et al., 2017). The Archean granitoids (inliers) studied here are in the Neoproterozoic Southern Brasília Orogen.

The Southern São Francisco Craton hosts a major Brazilian Fe mining district, known as the Quadrilátero Ferrífero (Iron Quadrangle; Fig. 1). It consists of amphibolite-facies granitoid-gneiss terrains (locally migmatitic) overlain by greenschist to amphibolite facies (locally high-grade) supracrustal sequences, in a dome and keel geometry (Alkmim and Marshak, 1998) likely established by the Neoarchean (Cutts et al., 2019). The supracrustal sequences include Archean greenstone belts (e.g., Rio das Velhas and Pitangui) and Paleoproterozoic metasedimentary and volcano-sedimentary units (Hartmann et al., 2006; Baltazar and Zucchetti, 2007; Farina et al., 2016; Moreira et al., 2016; Dopico et al., 2017; Brando-Soares et al., 2017, 2020).

The metagranitoid-gneisses of the Quadrilatero Ferrífero basement (Bação, Belo-Horizonte, Caeté, Santa Bárbara and Bonfim complexes) predominantly crop out in the core of domal structures. Four stages of magmatic activity have been identified, from 3220 Ma to 2610 Ma (Lana et al., 2013; Romano et al., 2013; Farina et al., 2015, 2016). The first is a short-lived TTG-dominated pulse in the Santa Bárbara Complex with an age of 3220–3200 Ma (Santa Bárbara event). Two magmatic pulses then occurred between 2930–2850 Ma and 2800–2760 Ma (the Rio das Velhas I and II events, respectively). Renewed magmatic activity between 2750 Ma and 2610 Ma, called the Mamona event, is represented by high-K metagranitoid plutons, which are weakly foliated to undeformed (Lana et al., 2013; Romano et al., 2013; Farina et al., 2015). Medium-K metagranitoids of the Rio das Velhas I and II events have higher K_2O and incompatible element contents (Rb, Th, U) than average TTG (Farina et al., 2015). Hence, it has been argued that these rocks formed as mixtures between a TTG melt, produced by partial melting of mafic crust, and melt derived by reworking of felsic continental crust (Farina et al., 2015). The presence of older crustal material in the generation of the Rio das Velhas I and II rocks is corroborated by negative $\varepsilon_{Hf}(t)$ of zircon crystals extracted from orthogneisses of the Quadrilátero region (Albert et al., 2016).

To the southwest of the Quadrilátero Ferrífero, close to the boundary with the Southern Brasília Orogen (studied area;

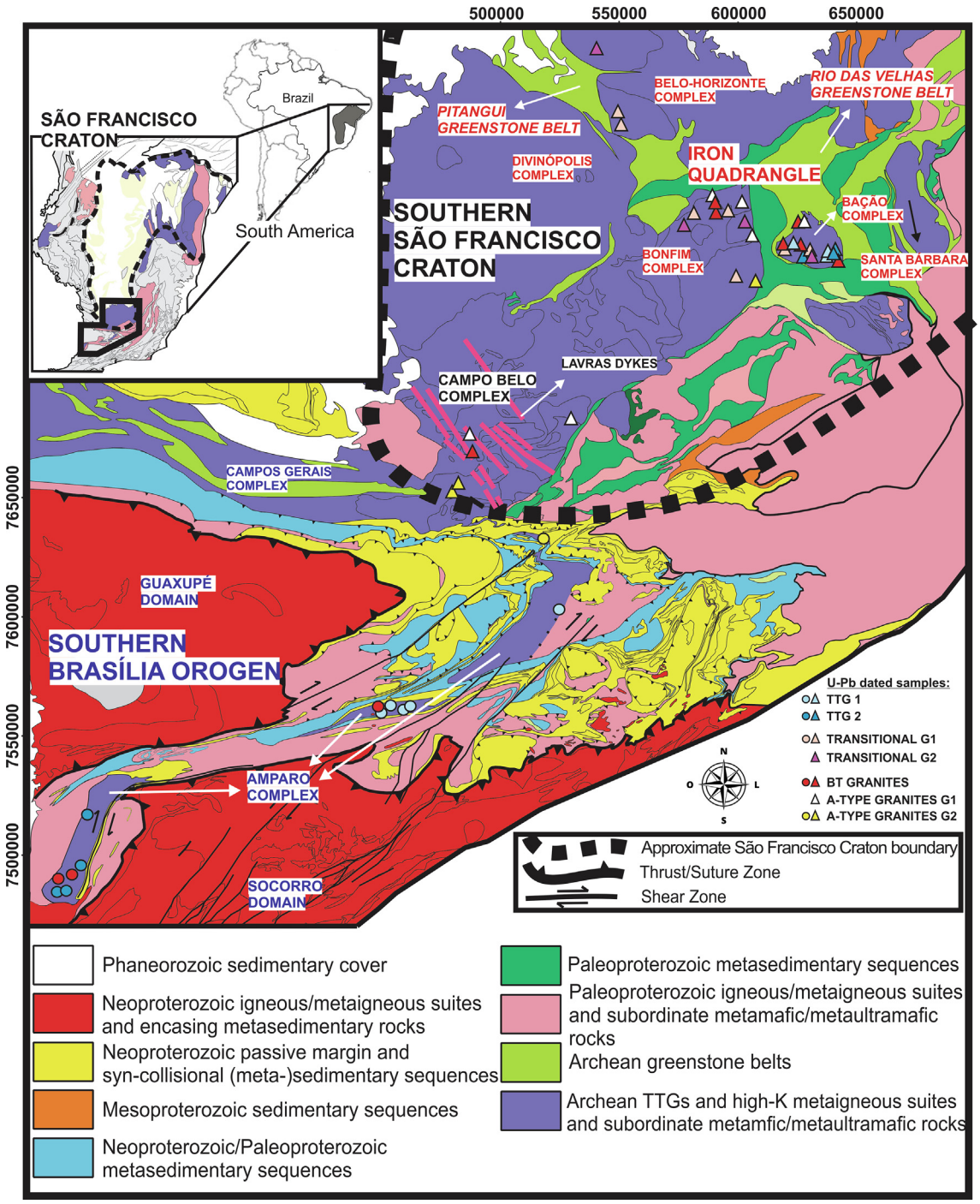

Fig. 1. Map of the southern portion of the Southern Brasília Orogen (adapted and modified from Campos Neto et al., 2011; Kuster et al., 2020 and references therein; Vinagre et al., 2020 and references therein) and the Southern São Francisco Craton (from Simon et al., 2021 and references therein). Samples for which U–Pb ages and geochemistry data are available are plotted, including those obtained in this study. Triangles represent samples from the Southern São Francisco Craton (Farina et al., 2015; Moreno et al., 2017), whereas spheres represent samples from the Southern Brasília Orogen (this study; Cioffi et al., 2016a).

Fig. 1), there is a large orthogneiss-dominated terrain, known as the Campo Belo Complex (e.g., Teixeira et al., 1996, 1998). Early studies (Teixeira et al., 1998) found evidence for three thermal episodes in the Campo Belo Complex, recorded in a polyphase migmatite: 3205 ± 17 Ma, 3047 ± 25 Ma and 2839 ± 17 Ma. Subsequently, Moreno et al. (2017) reported A-type-like granitoids and leucogranites dated between 2.73 Ga and 2.65 Ga in the Campo Belo Complex.

The Southern São Francisco Craton is marked by widespread high-K granites attributed to crustal anatexis (e.g., Romano et al., 2013; Farina et al., 2015), accompanied by metamorphic resetting of zircon grains and high-grade metamorphism (8–9 kbar; 650–700 °C) between ~2.85 Ga and 2.70 Ga (e.g., Lana et al., 2013; Cutts et al., 2019), and perhaps linked to crustal thickening (Cutts et al., 2019). It has been interpreted as a protracted period of sequential continental collisions (Lana et al., 2013; Farina et al., 2015; Albert et al., 2016; Aguilar et al., 2017), punctuated by arc/accretionary processes (e.g., Brando-Soares et al., 2020). Younger ages related to metamorphic overprint, between 2.68 Ga and ~2.6 Ga (concomitant with the Mamona event), are reported

by Campos et al. (2003), Farina et al. (2015) and Aguilar et al. (2017) and they may represent a period of post-collisional regional extension, followed by magmatism and renewed metamorphism (Albert et al., 2016). Although P–T conditions for this time period have yet to be investigated, mafic dyke swarms indicate crustal extension at ~2.55 Ga (e.g., Caxito et al., 2020). Finally, around the margins of Archean cratonic nuclei, there was crustal reworking and juvenile crustal addition between ~2.4 Ga and 2.0 Ga (e.g., Noce et al., 1998; Ávila et al., 2010, 2014; Teixeira et al., 2015, 2017). These are thought to be related to a younger tectonic cycle and are beyond the scope of this contribution.

2.2. Basement rocks of the Southern Brasilia Orogen and links with the São Francisco Craton

The Southern Brasilia Orogen is a Neoproterozoic fold and thrust system that borders the São Francisco Craton (Fig. 1; Valeriano et al., 2008; Campos Neto et al., 2011; Trouw et al., 2013; Marimon et al., 2020a, 2020b, 2021). Peak metamorphic conditions were attained between ~625–600 Ma, which resulted from a Brasiliano/Pan African orogenic event involving continent–continent collision of two major blocks (e.g., Trouw et al., 2013; Vinagre et al., 2014; Coelho et al., 2017; Marimon et al., 2021). Paleoproterozoic (Pouso Alegre Complex) and Archean basement of the Southern Brasília Orogen are preserved in a 300 km tectonic window between the Socorro and Guaxupé domains, and they are related to the adjacent São Francisco Craton (Cioffi et al., 2016a, 2016b).

The Archean basement of the Southern Brasilia Orogen is exposed in three distinct, unconnected locations in the nuclei of large antiformal fold structures (Fig. 1). In the western segment, adjacent to the Paraná basin, there are Meso-Neoarchean orthogneisses and migmatites (metatexites and diatexites) of TTG and high-K affinity (Cioffi et al., 2016a; Oliveira et al., 2019; Fontainha et al., 2021). This segment has been divided into the Amparo and Serra Negra complexes (e.g., Cioffi et al., 2016a and references therein). At the central portion of the belt, surrounding Heliodora town, Archean rocks form the core of a >30 km wide anticline, and the predominant rock-types comprise Mesoarchean Na-rich suites, partially mylonitized and migmatized (Cioffi et al., 2016a). The third Archean segment lies to the northeast, near Carrancas town, and it is composed of sodic orthogneisses, metagranites and metamafic/metaultramafic bodies, which are mostly migmatized (Santos, 2014). The central and northeastern Archean sections (Fig. 1) have been named the Heliodora-Minduri complex (e.g., Cioffi et al., 2016a and references therein). However, we consider the subdivision of Archean rocks in the Southern Brasília Orogen into different complexes to be unnecessarily complicated. The rocks are similar in terms of ages, mineralogy and composition, and thus we propose these Archean rocks be collectively known as the Amparo Complex.

The timing of when the Amparo Complex (this study) and the Southern São Francisco Craton amalgamated is difficult to constrain due to the polymetamorphic evolution of the considered regions. Cioffi et al. (2016a) speculated that it occurred at either ~2.0 Ga or ~2.7 Ga. The Amparo Complex is intruded by Paleoproterozoic high-K, isotopically evolved, metaigneous rocks with magmatic arc geochemical signatures (e.g., Oliveira et al., 2019) and overlain by juvenile Paleoproterozoic metaigneous rocks (Cioffi et al., 2016b) that are probably allochthonous. This suggests that a continental arc was established at the border of the Archean São Francisco proto-continent during the Paleoproterozoic, with the accretion of exotic terranes (island arcs?) thrust over the Archean basement, now exposed within the Southern Brasília Orogen. Thus it appears that the Amparo Complex had already coalesced with the São Francisco Craton at the Paleoproterozoic.

However, there is also some evidence that the Southern São Francisco Craton and the basement of the Southern Brasília Orogen (i.e., Amparo and Campos Gerais complexes) were accreted in the Neoarchean (~2.8–2.7 Ga) during a period of major crustal reworking and partial melting of TTG in both regions, which generated large volumes of biotite granites (Romano et al., 2013; Farina et al., 2015; Albert et al., 2016; Cioffi et al., 2016a, 2016b; Valeriano et al., 2022). TTG magmatism between 3.05 Ga and 2.95 Ga is common in the basement of the Southern Brasília Orogen but it is rare in the Southern São Francisco Craton (e.g., Farina et al., 2015; Simon et al., 2021). Therefore, it is reasonable to assume that a segment of Archean crust, represented by the basement of the Southern Brasília Orogen (Fig. 1) to the southwest, collided with a block to the northeast, represented by the Southern São Francisco Craton (Fig. 1), during the Neoarchean (e.g., Cioffi et al., 2016a, 2016b). However, 3.05–2.95 Ga TTG in the Southern São Francisco Craton may have been reworked during the Neoarchean metamorphic event, as inherited zircon grains of 3.10 Ga and 2.95 Ga are found in younger granites (Simon et al., 2021). In this contribution we discuss newly obtained data from the Southern Brasília Orogen's Archean basement in conjunction with compiled data from the Southern São Francisco Craton. However, we treat the datasets independently given the possibility that these regions evolved separately during the Archean.

3. Petrology and field relations

In the Amparo Complex, the Archean basement of the Southern Brasília Orogen (Fig. 1), lithologic units can be subdivided into four groups, on the basis of field and thin section analyses (Fig. 2), which are further constrained geochemically in the following section. We note that most of the studied Archean igneous/metaigneous rocks are stromatic migmatites, with thin banding (cm-scale leucossomes and mm-scale melanossomes; Fig. 2). Diatexites were avoided for geochemical analyses due to likely element mobility, and only outcrops with incipient-to-moderate or no migmatization were sampled for analysis. Some outcrops were formed entirely by thinly banded stromatic migmatites, whereupon large samples were collected to evaluate the rock's composition prior to migmatization (e.g., Fig. 2C).

Two groups of low-K orthogneisses (tonalitic, trondhjemitic and granodioritic: TTG), were recognized: TTG 1 and TTG 2 (Fig. 2). TTG 1 rocks are characterized by lower contents of ferro-magnesian minerals than TTG 2 (Fig. 2), and TTG 1 are mostly fine- to medium-grained trondhjemites (Fig. 2A and B), with plagioclase, quartz and biotite as major rock-forming minerals and apatite, (±) allanite and zircon as accessory minerals. TTG 2 are mostly medium-grained tonalites (Fig. 2C and D) with plagioclase, quartz, biotite, hornblende and minor-to-absent (±) K-feldspar as constituent minerals, as well as titanite, opaques, allanite and zircon as accessory phases. In both TTG groups, chlorite, muscovite and epidote are common alteration products.

Three groups of high-K rocks were recognized during field mapping and thin section analyses. The first two groups, the biotite-two-mica granites (BTMG) and the transitional granites (TRAN. G1), are similar and are hard to distinguish in the field (Fig. 2E, F and G). They are formed by abundant K-feldspar, plagioclase and biotite as major minerals, although BTMG samples have higher K-feldspar contents than TRAN.G1. The common accessory minerals are titanite, allanite, epidote, zircon, apatite and opaque minerals, and primary muscovite is present in a couple of samples of peraluminous granites belonging to the BTMG group.

The third group of high-K rocks is easily distinguished as the granites are porphyritic and richer in ferromagnesian minerals. In the Amparo Complex (south of Itumirim town), it is represented

Fig. 2. Hand samples of analyzed rocks from the Amparo Complex, Southern Brasília Orogen.

by sample CAR, which is a porphyritic granite (Fig. 2H) with K-feldspar, plagioclase, quartz, biotite and hornblende, as well as accessory epidote and zircon. This group of rocks is also recognized in the São Francisco Craton (e.g., Lavras Granitoid of Moreno et al., 2017) and it has been called A-type Group 2 based on geochemical criteria (Section 4).

4. Whole-rock geochemistry

Major element analyses were initially used to subdivide the 32 analyzed granitoid samples from the basement inliers of the Southern Brasília Orogen, and the 66 published analyses from the Southern São Francisco Craton, into three broad groups: TTG, transitional granitoids and granites. Significant subgroups were subsequently recognized based on major and trace element contents and the subgroups A-type granites group 1 (AGG1) and transitional granitoids group 2 (TRAN.G2) were only recognized for rocks of the Southern São Francisco Craton (for more information on mineralogy the reader is referred to Farina et al., 2015). A complete geochemical data spreadsheet, with compiled and new analyses, is provided in Supplementary Material 1.

Granitoid samples that have K_2O/Na_2O values <0.5, and which plot in the trondhjemite and tonalite fields in the O'Connor (1965) diagram (Fig. 3A), and the TTG field in the Na_2O/K_2O-2A/CNK-2FMSB diagram of Laurent et al. (2014a) (Fig. 3B), were classified as TTG. These samples were further subdivided into TTG 1 and TTG 2 on the basis of selected major and trace elements, as well as distinct mineralogical compositions as discussed in the previous section (i.e., higher contents of ferromagnesian minerals and the presence of hornblende in TTG 2). TTG 1 are HREE poor and have higher La/Yb and Sr/Y, and lower Yb and Rb/Al_2O_3 than TTG 2 (Fig. 4). The subdivision between TTG 1 and TTG 2 is arbitrary and overall the TTG comprise a compositional continuum, with some overlap, rather than two readily distinguished subgroups. TTG 2 have higher FeO_t + MgO + MnO + TiO_2 and CaO, and both compatible (e.g., Cr, V and Ni; Supplementary Material 1; Supplementary Material 2, Fig. S6) and incompatible HFSE trace elements than TTG 1 (e.g., Th, Nb, Ta, Zr and Hf; Supplementary Material 1). TTG 2 have negative anomalies of Sr and Eu in normalized multi-

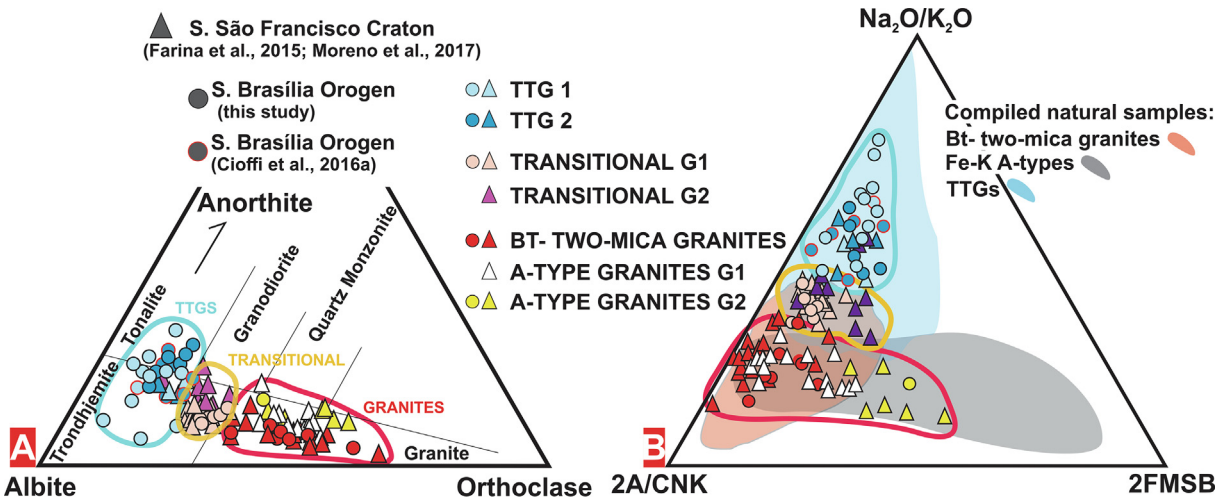

Fig. 3. O'Connor (1965) classification diagram (A), and the ternary discrimination diagram (B) of Laurent et al. (2014a). Triangles represent samples from the Southern São Francisco Craton, and circles are samples from the Southern Brasília Orogen. Fields of mostly Archean natural samples are also present (compiled natural samples). Published TTG analyses (n = 1478, light blue field) are from Moyen (2011) and references therein. Archean biotite and two-micas granites (n = 157, red field) were compiled from Mikkola et al. (2012) and references therein and Laurent et al. (2014a) and references therein. A-type granitoids (n = 203, light grey field) are mostly of Archean age (Sardinha et al., 2006; Dall'Agnol and Oliveira, 2007; Laurent et al., 2014b; Zhou et al., 2015; Marangoanha et al., 2019; Savko et al., 2019), with the exception of the data from Vander Auwera et al. (2003).

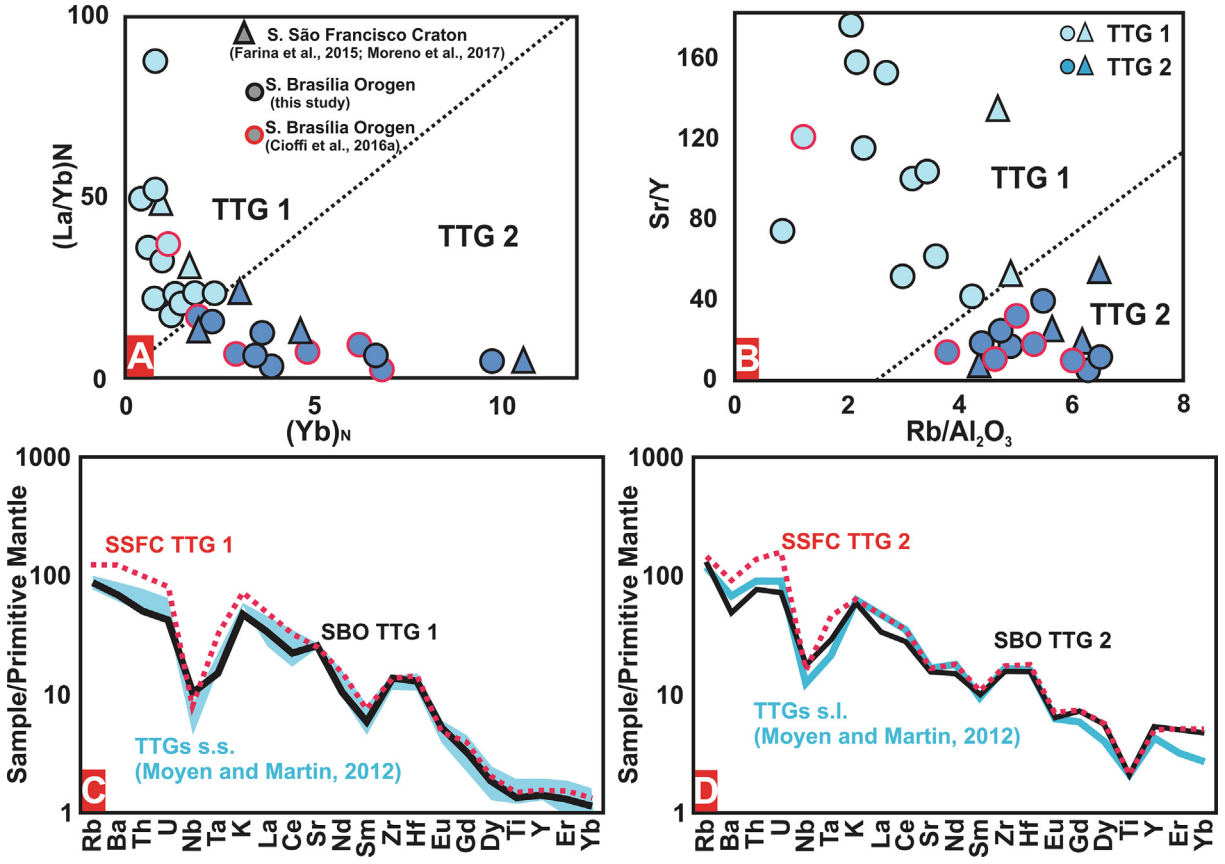

Fig. 4. Diagrams: $(La/Yb)_N$ versus $(Yb)_N$ (A) and Sr/Y versus Rb/Al_2O_3 (B). (C and D) Multielement spider diagrams of the average Archean TTG orthogneiss composition from the Southern Brasília Orogen (SBO; this study; Cioffi et al., 2016a) normalized to primitive mantle composition (McDonough and Sun, 1995). For comparison, the mean of samples from the Southern São Francisco Craton (SSFC; Farina et al., 2015) are plotted as dotted lines.

element plots, whereas TTG 1 are characterized by positive (or the absence of) anomalies for these elements (compare Fig. 4C and D). Negative Nb-Ta anomalies are a feature of both TTG groups, but negative Ba anomalies are more common in the TTG 2 samples (Fig. 4C and D).

Transitional granitoids, which are medium-K rocks (K_2O/Na_2O = 0.5–0.8), have compositions intermediate between those of the trondhjemite and granite fields in the O'Connor (1965) (Fig. 3A) diagram and the TTG and biotite- two-mica granite fields in Fig. 3B. Transitional granitoids are richer in K_2O (and K-feldspar)

compared to TTGs and they were further subdivided into two groups. The transitional granitoids group 1 (TRAN.G1) have lower FeO_t + MgO + TiO_2 + MnO, Th, U and HFSEs and higher Rb and Sr compared with transitional granitoids group 2 (TRAN.G2) (Figs. 3B and 5A). One of the most striking differences between TRAN.G1 and TRAN.G2 samples is in the sum of the REE which tends to be considerably higher in TRAN.G2 (238 ppm), similar to the average sanukitoid of Laurent et al. (2014a) (Fig. 5A). The TRAN.G1 and TRAN.G2 are readily distinguished on multi-element spider plots (Fig. 5A), since they form markedly different patterns and intermediate compositions between the two groups are absent. In more detail the marked negative Sr anomaly of the average TRAN.G2 contrasts with the slightly positive one of the average TRAN.G1 (Fig. 5A). It is important to highlight that as yet no TRAN.G2 have been found in the Southern Brasília Orogen (this study) and this discussion is based on samples from the Southern São Francisco Craton (Farina et al., 2015). A couple of analyses that have K_2O/Na_2O values lower than 0.5 and that plot on the TTG field in Fig. 3B, have very high HFSE contents and they were therefore considered as TRAN.G2 and not TTG.

At the other end of the compositional spectrum, high-K granites (K_2O/Na_2O >0.8; red, white and yellow symbols in Fig. 3) plot in the granite field in the O'Connor (1965) diagram and in the area of overlap between the biotite- two-mica granite and A-type fields in the Na_2O/K_2O-2A/CNK-2FMSB figure in Fig. 3B. The latter is part of the sanukitoid *sensu lato* field of Laurent et al. (2014a), since the definition of sanukitoid *sensu lato* encompass sanukitoids *sensu stricto* and some A-types which are thought to have similar petrogenetic processes (Laurent et al., 2014a, 2014b). However, we have subdivided the sanukitoid *sensu lato* group (Laurent et al., 2014a) because it includes A-type granites which, as discussed later, appear to have distinct origins. Sanukitoids *sensu stricto* (e.g., Heilimo et al., 2010) are compositionally distinct from A-types in that ferroan A-types (e.g., Eby, 1992; Frost and Frost, 1997, 2011; Dall'Agnol et al., 2005) have higher FeO_t, TiO_2, HFSEs and lower MgO contents than magnesian sanukitoids *sensu stricto* (e.g., Heilimo et al., 2010; Laurent et al., 2011).

The fields of A-types and biotite- two-mica granites significantly overlap in the Na_2O/K_2O-2A/CNK-2FMSB diagram (Fig. 3B). However, these groups can be separated based on the higher FeO_t/MgO, FeO_t + MgO + TiO_2 + MnO, HFSE, TiO_2 and lower contents of Al_2O_3 of the A-types (Fig. 5B, C and D; Supplementary Material 2, Fig. S5). This is most marked in Fig. 5C, where there is no overlap between the fields for the A-types and biotite- two-mica granites. In addition, since A-types have much higher HFSE contents than the biotite- two-mica granites, mantle-normalised plots readily distinguish the two groups (Fig. 5B). A-type granites were further subdivided into group 1 (A-type granites G1; AGG1) and 2 (A-type granites G2; AGG2) according to the lower Al_2O_3, Th, U, Rb, LREE, and higher $FeO_t/(FeO_t$ + MgO), TiO_2, Ba, Zr and total ferromagnesian oxides of the latter compared with the former (Supplementary Material 1; Fig. 5B, C and D). Based on these differences, the classification diagrams of Fig. 5C and D were constructed, and they separate AGG1 and AGG2 samples, since they plot in different fields with little overlap. It must be clarified that this classification is distinct from the A1/A2 classification of Eby (1992). AGG1 samples are yet to be found in the Southern Brasília Orogen, and so the samples discussed here are from the Southern São Francisco Craton (Farina et al., 2015; Moreno et al., 2017).

5. Zircon U–Pb and Lu–Hf, and whole-rock Sm–Nd

A number of samples from the Amparo Complex, Southern Brasília Orogen, were selected for U–Pb, Lu–Hf and Sm–Nd analyses. U–Pb zircon magma crystallization ages are shown as red squares in the Wetherill diagrams in Fig. S3 of Supplementary Material 2, and the zircon ages interpreted as metamorphic (low Th/U overgrowths and homogenous grains) are plotted as blue squares. The Lu-Hf data are presented in Fig. 6, together with data obtained by Albert et al. (2016) for the Southern São Francisco Craton. Sm-Nd data obtained in this study is shown in Supplementary Material 3, as well as in Fig. S4 of Supplementary Material 2. More information on the U–Pb (LA-ICP-MS and ID-TIMS), Lu–Hf and Sm–Nd methodology, as well as descriptions of cathodoluminescence-supported zircon age interpretations for each dated sample, and a discussion of the criteria used for the recognition of metamorphic or crystallization ages, is available in Supplementary Material 2. For complete tables on the U–Pb, Lu–Hf and Sm–Nd data obtained in this study the reader is referred to Supplementary Material 3.

The five analyzed TTG samples yielded zircon U–Pb crystallization ages between 3024 ± 9 Ma and 2946 ± 10 Ma (Supplementary Material 2, Fig. S3), and high-K biotite- two-mica granite samples (BTMG; n = 3) have U–Pb discordia ages between 2798 ± 9 Ma and 2729 ± 13 Ma (Supplementary Material 2, Fig. S3). The youngest dated sample (2705 ± 5 Ma) is from the AGG2 group. Most of the analyzed TTG samples have Hf (Fig. 6) and Nd initial isotope ratios that plot close to or above the CHUR (between +1.41 and −1.81 $\varepsilon_{Hf}(t)$) and some are close to or slightly above DM (between +5 and +9 $\varepsilon_{Hf}(t)$; Supplementary Material 2, Fig. S4). Thus, they represent relatively new additions to the crust and/or reworking of crust recently extracted from the mantle. In contrast, the high-K BTMG and AGG2 samples tend to have negative εHf and εNd values, and they plot on crustal evolution isotope arrays with the TTG, which indicates reworking of older crustal material during the generation of these high-K rocks (Supplementary Material 2, Fig. S4).

Metamorphic U–Pb zircon ages range from 2880 ± 8 Ma (based on zircon overgrowths; Supplementary Material 2, Fig. S3I), to 2721 ± 23 Ma (homogenous metamorphic zircon grains; Supplementary Material 2, Fig. S3G), and a Paleoproterozoic metamorphic event at 2079 ± 11 Ma (zircon overgrowths; Supplementary Material 2, Fig. S3E).

6. Chemical changes through time

There are marked differences in the geochemistry of granitoid rocks of different U–Pb ages (Figs. 6 and 7). K_2O/Na_2O and Rb/Sr ratios increase with decreasing ages (Fig. 7A–B) highlighting the shift to more granitic lithologies, and the progressive maturation of the Archean continental crust of the Southern São Francisco Craton and Southern Brasília Orogen. The highest Rb/Sr values occur at ~2.72 Ga, concomitant with the largest peak in the probability density plot of the metamorphic ages (green) from the Southern São Francisco Craton (Fig. 7B). Th/Nb ratios in mafic rocks are regarded as indicative of tectonic setting (Pearce, 2008), and in granitic rocks they may reflect the Th/Nb ratios of their crustal source rocks, and/or the effects of rutile, allanite, apatite, monazite and/or ilmenite during petrogenesis. Th/Nb increases progressively from ~3.0 Ga to ~2.68 Ga, before decreasing in the late higher-Nb A-type granites group 2 (Fig. 7C). These geochemical changes through time are linked to progressive crustal reworking, after a period of predominantly juvenile TTG production, as evidenced by the Lu–Hf data (Fig. 6). If we consider the Southern São Francisco Craton and the Southern Brasília Orogen separately, the exposed trends would still be valid, albeit the trends of the Brasília Orogen are better delineated due to a larger age range.

After ~2.7 Ga, the crustal record is marked by the appearance of limited volumes of granites with high FeO_t/MgO, Ba/Rb and TiO_2, but low Al_2O_3, and they are classified as A-types granites group 2 (Fig. 7D). Rocks from this group are set apart from all other groups

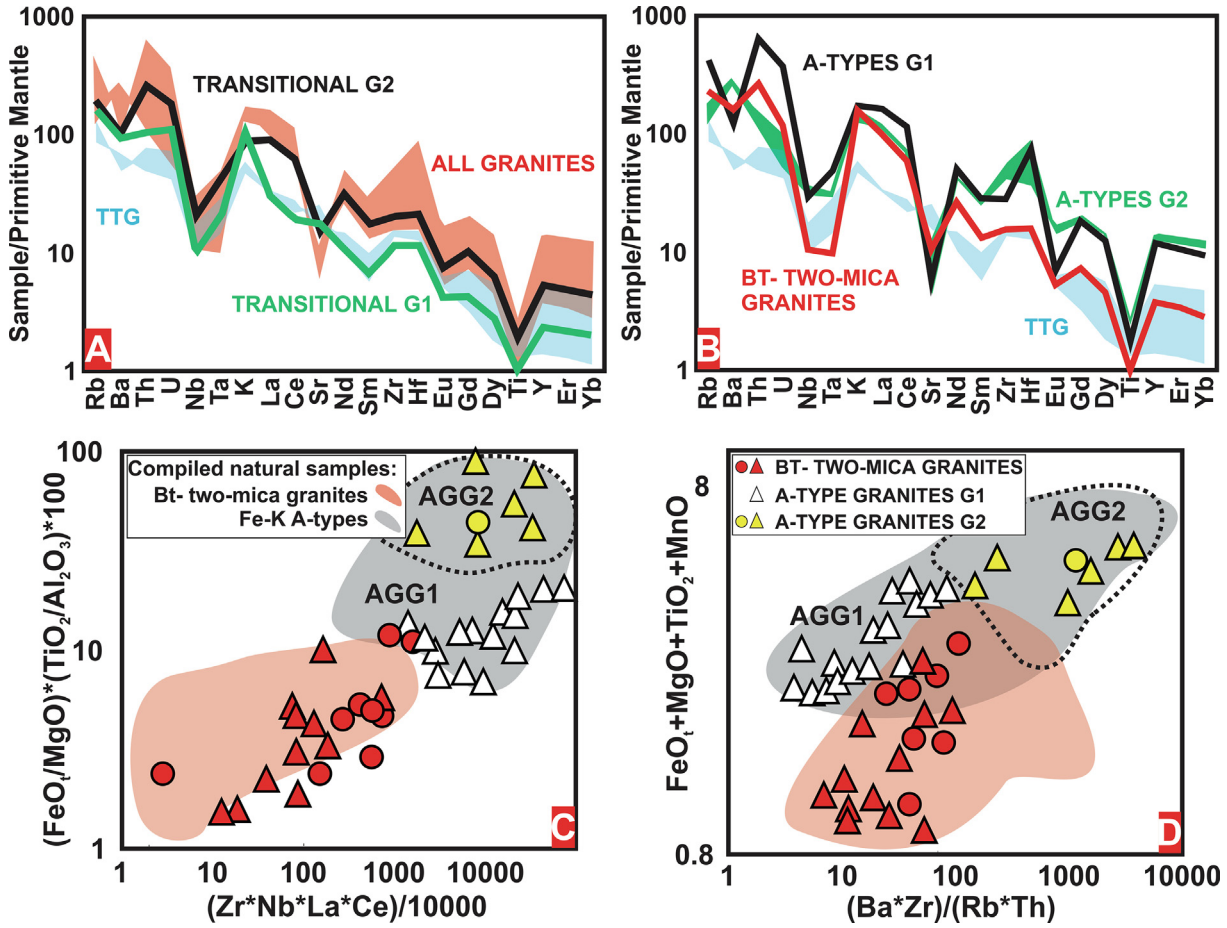

Fig. 5. Multielement spider diagrams (A and B) show the average composition of the considered Archean orthogneisses' geochemical groups, which are normalized to primitive mantle composition (McDonough and Sun, 1995). The TTG fields (blue in A and B) are constructed based on the average TTG 1 and 2 compositions. The green field in B, representing A-type granites G2, was drawn based on the average A-type G2 composition from the Southern São Francisco Craton and sample CAR (AGG2), from the Southern Brasília Orogen. $(FeO_t/MgO)*(TiO_2/Al_2O_3)*100$ versus $(Zr*Nb*La*Ce)/10000$ (C) and $FeO_t + MgO + TiO_2 + MnO$ versus $(Ba*Zr)/(Rb*Th)$ diagram (D). Samples from the Southern Brasília Orogen (this study; Cioffi et al., 2016a) and Southern São Francisco Craton (Farina et al., 2015; Moreno et al., 2017) are plotted.

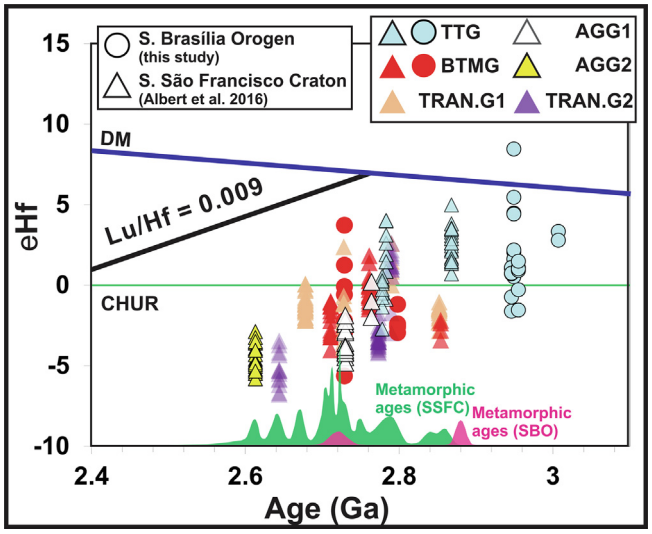

Fig. 6. Age versus $\varepsilon_{Hf}(t)$ diagram with metaigneous samples from the Southern Brasília Orogen (spheres; this study) and the Southern São Francisco Craton plotted (triangles; Albert et al., 2016). BTMG = biotite- two-mica granites; TRAN.G = transitional granitoids groups 1 and 2; AGG1 = A-type granites group 1; AGG2 = A-type granites group 2.

in Fig. 7D, due to their distinctive geochemistry and because they were emplaced late in the magmatic record.

Nb/Ta is regarded as a pressure proxy, with Nb/Ta increasing with increasing pressure (Foley et al., 2002), although this must be viewed with caution as the source composition and differentiation processes can also influence Nb/Ta (e.g., Moyen and Laurent, 2018). Nb/Ta in the TTG decreases from 3.0 Ga to ~2.78 Ga, and between ~2.80 Ga and 2.75 Ga, three granite samples have the lowest recorded Nb/Ta values (Fig. 7E). Overall, there is a weak V-shaped pattern with Nb/Ta values decreasing from 3.0 Ga to 2.80–2.78 Ga and then slightly increasing afterwards (Fig. 7E). Dy/Yb is controlled by the crystallization and/or residual presence of garnet and/or amphibole (e.g., Davidson et al., 2013), and it is widely used as an indicator of the depths of magma petrogenesis (e.g., Moyen, 2011). However, there are no clear systematic changes in Dy/Yb with age in the granitic rocks in Fig. 7F.

7. Discussion

Batch melting models were used to evaluate the source rocks and the residual mineralogy during the generation of the different granitoids. Most of the geochemical groups have a restricted silica range, and although samples with the lowest silica contents were considered during modelling, they tend not to vary significantly from the average values and when they do, this can be readily explained by varying conditions during partial melting (e.g., pres-

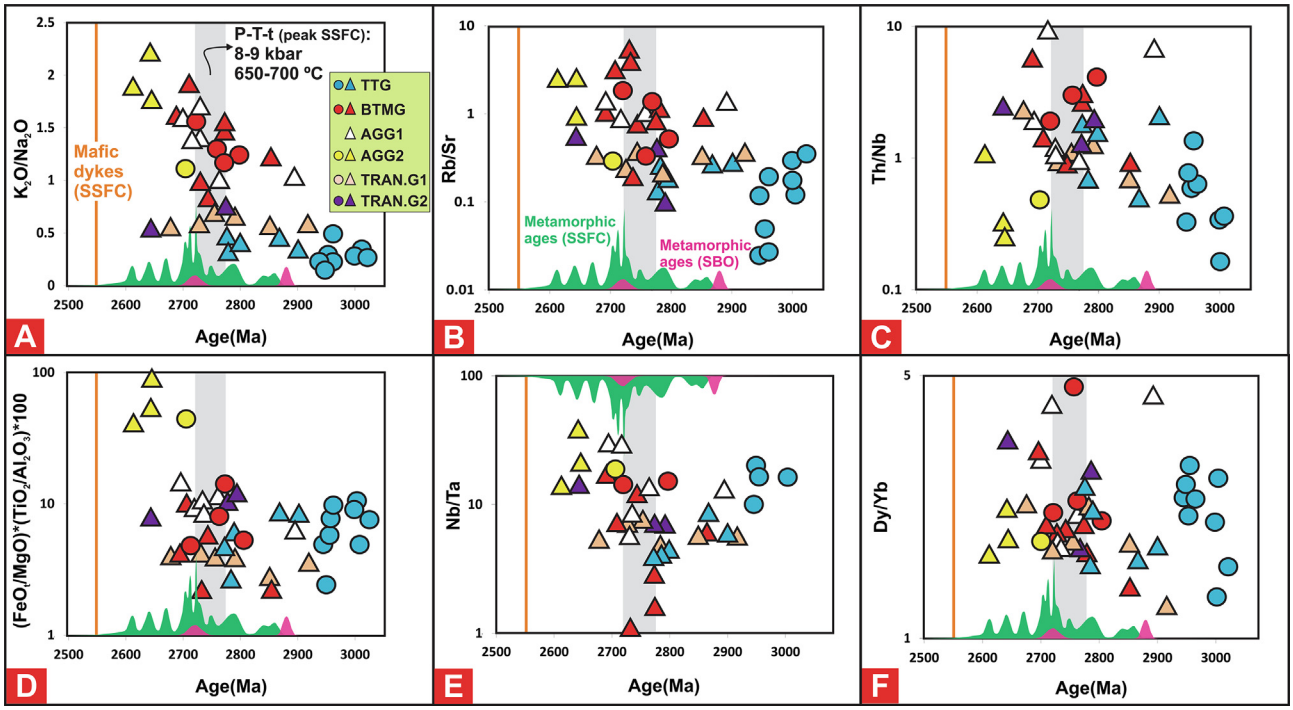

Fig. 7. Selected geochemical ratios versus time. All vertical scales are log, with the exception of (A). Grey bars indicate the timing of measured P–T conditions by Cutts et al. (2019). Data from the Southern Brasília Orogen (circles) are from this study and from Cioffi et al. (2016a), whereas samples from the Southern São Francisco Craton (triangles) are from Farina et al. (2015) and Moreno et al. (2017). Probability density plots (green and purple) represent U–Pb zircon (overgrowth, soccer-ball grains, etc.) and monazite metamorphic ages obtained from the Southern São Francisco Craton (n = 21; the reader is referred to Supplementary Material 4 for references) and the Southern Brasília Orogen (n = 2; this study). The age of mafic dykes represented as an orange bar are from Caxito et al. (2020).

sure, melt content, temperature, etc). This approach is warranted by field and petrographic observations. No evidence of extensive crystal accumulation has been observed, whereas partial melting, with varying melt proportions at different locations, is present throughout the Amparo Complex, in both outcrop and thin section scale. Furthermore, partial melting has long been considered one of the dominant driving processes of crustal chemical differentiation (e.g., Sawyer et al., 2011). Together with age and isotopic data, the results of the melting models are then used to evaluate the geodynamic scenarios in which the magmas were generated. Rayleigh fractionation/melting models were also considered, but these yielded less consistent results and they are not discussed further. More information on the applied batch (equilibrium) melting/crystallization formula is given in Supplementary Material 2 and the partition coefficients used are in Supplementary Material 5.

7.1. Petrogenesis

7.1.1. TTg

This section explores the generation of the TTG (trondhjemites-tonalites-granodiorites), suites of low-K igneous rocks that typify much of the Archean continental crust (e.g., Moyen and Martin, 2012). These rocks are widely thought to have been derived from parent rocks of basaltic composition (e.g., Rapp and Watson, 1995), and possible mafic source rocks of similar age to the TTG crop out in the greenstone belts of the Southern São Francisco Craton (e.g., Brando-Soares et al., 2020). Mafic rocks dominate the lower stratigraphic segments of the greenstones (e.g., Moreira et al., 2016) and they include suitable source rocks for the TTG of the Southern São Francisco Craton. Batch melting calculations are used to constrain the trace and major element compositions of source rocks for the different subgroups of the analyzed TTG by partial melting under distinct thermodynamic conditions, characterized by differences in restite mineralogy.

TTG *sensu strictu* (TTG 1, in this study), as described by Moyen and Martin (2012), are regarded as the result of partial melting of hydrous basalts metamorphosed into eclogite or garnet-bearing amphibolite (e.g., Martin, 1986, 1987; Smithies, 2000; Rapp et al., 2003), and experimental petrology has confirmed that melts of similar composition to natural TTG can be obtained by partial melting of basalts over a range of pressure and temperature conditions (e.g., Beard and Lofgren, 1991; Rapp et al., 1991; Rapp and Watson, 1995; Springer and Seck, 1997; Laurie and Stevens, 2012). Accordingly, the TTG considered in this study have major element compositions similar to those of the experimental melts of low-K mafic rocks (Fig. 8A and B).

The basaltic source rocks of the average Archean TTG tend to have had higher incompatible element abundances than MORB (Smithies et al., 2009; Martin et al., 2014; Johnson et al., 2017), and the mafic volcanic rocks of the Southern São Francisco Craton have LILE-enriched compositions. These mafic rocks are concentrated in the greenstone belts that surround granitoid complexes (Fig. 1; Verma et al., 2017; Brando-Soares et al., 2020) in a dome-and-keel geometry thought to have been formed in the Archean and reactivated during a Paleoproterozoic tectono-metamorphic event (e.g., Cutts et al., 2019). Felsic and mafic magmatism in the Rio das Velhas Greenstone Belt (Fig. 1) bracket the development of this volcano-sedimentary sequence between >2.95 Ga and 2.75 Ga (Machado et al., 1992; Noce, 2000, Noce et al., 2005; Lobato et al., 2001; Moreira et al., 2019), although part of the Rio das Velhas Greenstone Belt is older than ~2.95 Ga as it is intruded by a U–Pb dated granodiorite of that age (Moreira et al., 2019). Metabasalts from the Pitangui Greenstone Belt (Southern São Francisco Craton; Fig. 1), adjacent to the Belo Horizonte Complex of the Iron Quadrangle region (Fig. 1), yielded an upper-intercept discor-

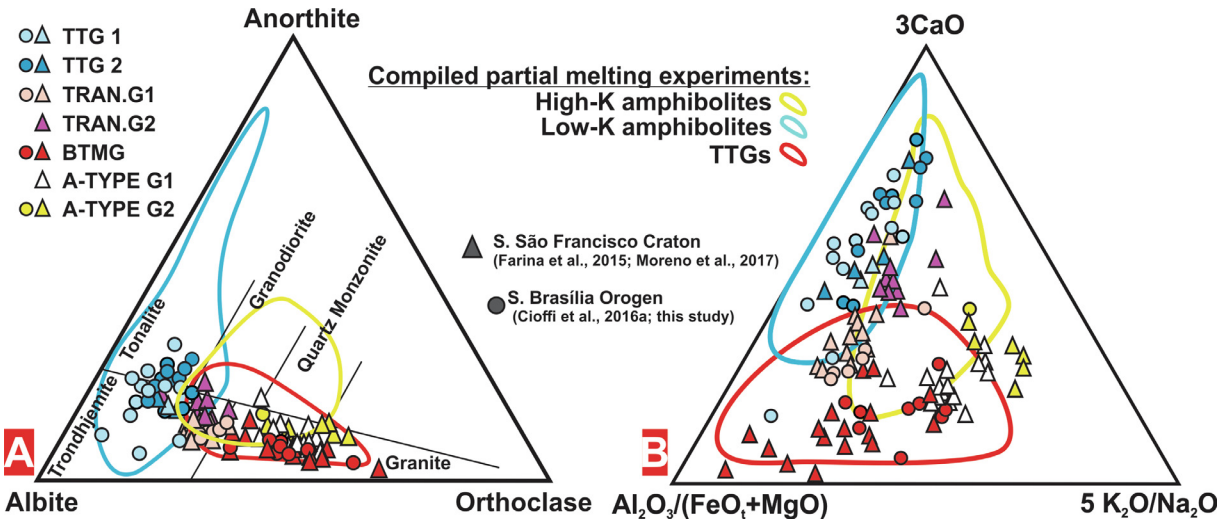

Fig. 8. Granitoid discrimination diagram of O'Connor (1965) (A) and ternary discrimination diagram of Laurent et al. (2014a) (B). Fields represent compiled partial melting experiments. Analyses of glasses (n = 91, yellow line) from partial melting experiments of high-K amphibolites (i.e. K_2O >0.7 wt.% and K_2O/Na_2O between 0.23 and 0.61) were compiled from Rapp et al. (1991, 1999), Sen and Dunn (1994), Patiño Douce and Beard (1995), Sisson et al. (2005) and Ye et al. (2021). Partial melting experiments of low-K amphibolites (K_2O < 0.8 wt.% and K_2O/Na_2O < 0.2; n = 175, blue line) are from Beard and Lofgren (1991), Rapp et al. (1991), Beard et al. (1994), Wolf and Wyllie (1994), Rapp and Watson (1995), Winther (1996) and Springer and Seck (1997). Major elements of glasses (n = 89, red line) from partial melting of TTGs were compiled from Skjerlie and Johnston (1992, 1993), Patiño Douce (1997, 2005), Patiño Douce and McCarthy (1998), Castro (2004) and Watkins et al. (2007).

dia U–Pb age of ~2.80, interpreted to represent crystallization age (Melo-Silva et al., 2020). Thus, magmatic events in these greenstone belts were broadly coeval with the TTG from the Southern São Francisco Craton (Farina et al., 2015; 2.91–2.77 Ga).

The TTG from the Southern São Francisco Craton have a restricted range in SiO_2 (71–72 wt.% for TTG 1 and 67–72 wt.% for TTG 2) and the trace element contents of the samples with the lowest SiO_2 are similar to the average of all the samples. Therefore, we model the averages of the TTG subgroups as partial melts, to smooth out outliers and to minimize the effects of analytical errors and/or metamorphic alteration. We applied trace-element batch melting calculations to the average basaltic (47–53 wt.% SiO_2) rocks from the Rio das Velhas and the Pitangui greenstone belts in the Southern São Francisco Craton (see Supplementary Material 6 for the selection of greenstone samples used in the batch melting calculations). The mineralogy of the restites, melt proportions (F) and P–T conditions are from the thermodynamic calculations of Palin et al. (2016). The authors used the average Archean tholeiitic basalt as starting material, which has a similar composition to the average mafic rock from the considered greenstone belts (Supplementary Material 2, Fig. S7).

Using the average mafic rock (47–53 wt.% SiO_2) composition of each greenstone belt, we reproduced the trace-element pattern of the TTG subgroups from the Southern São Francisco Craton (Supplementary Material 2, Fig. S7). The minerals that dominated the residual assemblage during formation of TTG 2 (6 kbar; 855 °C; F = 0.2) were hornblende, plagioclase, clinopyroxene and orthopyroxene, without garnet (Supplementary Material 2, Fig. S7C). In contrast, TTG 1 was better modelled at 12 kbar, 875 °C and F = 0.2 (from Palin et al., 2016) with a residual mineral assemblage with small amounts of plagioclase and with significant amounts of garnet, hornblende and clinopyroxene (Supplementary Material 2, Fig. S7B). The average composition of the Pitangui greenstone belt (Brando-Soares et al., 2020) better reproduced the TTG compositions of the Southern São Francisco Craton, although the TTG have slightly higher incompatible elements than the models, which could indicate assimilation of the crust during emplacement and/or limited fractional crystallization (Supplementary Material 2, Fig. S7).

The TTG of the Southern Brasília Orogen may have been emplaced in a distinct block separate from the TTG of the Southern São Francisco Craton, as discussed previously. Therefore, we used the average Archean basalt of Martin et al. (2014) as source to model the TTG from the Southern Brasília Orogen. Using parameters from Palin et al. (2016), we were able to perfectly match the trace and major element contents of the average TTG 1 (12 kbar; 875 °C; F = 0.2) and TTG 2 (6 kbar; 855 °C; F = 0.2) (Fig. 9). Again, the presence of large amounts of residual garnet and restricted plagioclase, accounts for the high Sr and La/Yb of the TTG 1, whereas the absence of garnet and the high contents of residual plagioclase produces a melt with composition similar to that of TTG 2 (Fig. 9). Since the silica contents vary considerably in the TTG of the Southern Brasília Orogen, we explored how the models compare to the samples with the lowest SiO_2 contents, from both subgroups. For trace element contents, the differences between the average TTG and the lowest silica TTG are very small (Fig. 9). However, the contents of FeO_t and MgO are higher in the samples with low SiO_2 and they were successfully reproduced by a ~50 °C increase in temperature and 10% increase in the melt content compared to the parameters used for modelling the average TTG (Fig. 9). Thus, variations in the conditions of partial melting accounts for most of the observed compositional variations in the TTG subgroups, without the need of pervasive fractional crystallization and assimilation. This is consistent with the absence of evidence for such processes and the abundant evidence for partial melting, at varying degrees, in the Amparo Complex of the Southern Brasília Orogen, which includes the presence of amphibolite rafts in the TTG.

The differences in the residual mineral assemblages of TTG 1 and 2 are widely attributed to different pressures during partial melting (e.g., Moyen, 2011; Palin et al., 2016). Garnet-rich and plagioclase-poor residue in equilibrium with a TTG 1 melt (Fig. 9) are taken to reflect higher pressure conditions (Moyen, 2011). In contrast, a garnet-poor and plagioclase-rich residue in equilibrium with a TTG 2 melt (Fig. 9) indicates lower crustal pressures (Moyen, 2011). However, recent studies (e.g., Halla, 2020; Laurent et al., 2020; Pourteau et al., 2020) have argued that the chemical diversity of TTG could reflect other processes, such as the availability of fluids, rather than the depth of partial melting (Palin et al., 2016; Pourteau et al., 2020; Hernández-Montenegro et al., 2021).

Although hydrated sources, i.e., minimum water saturation, are thought to be essential for voluminous TTG production (e.g.,

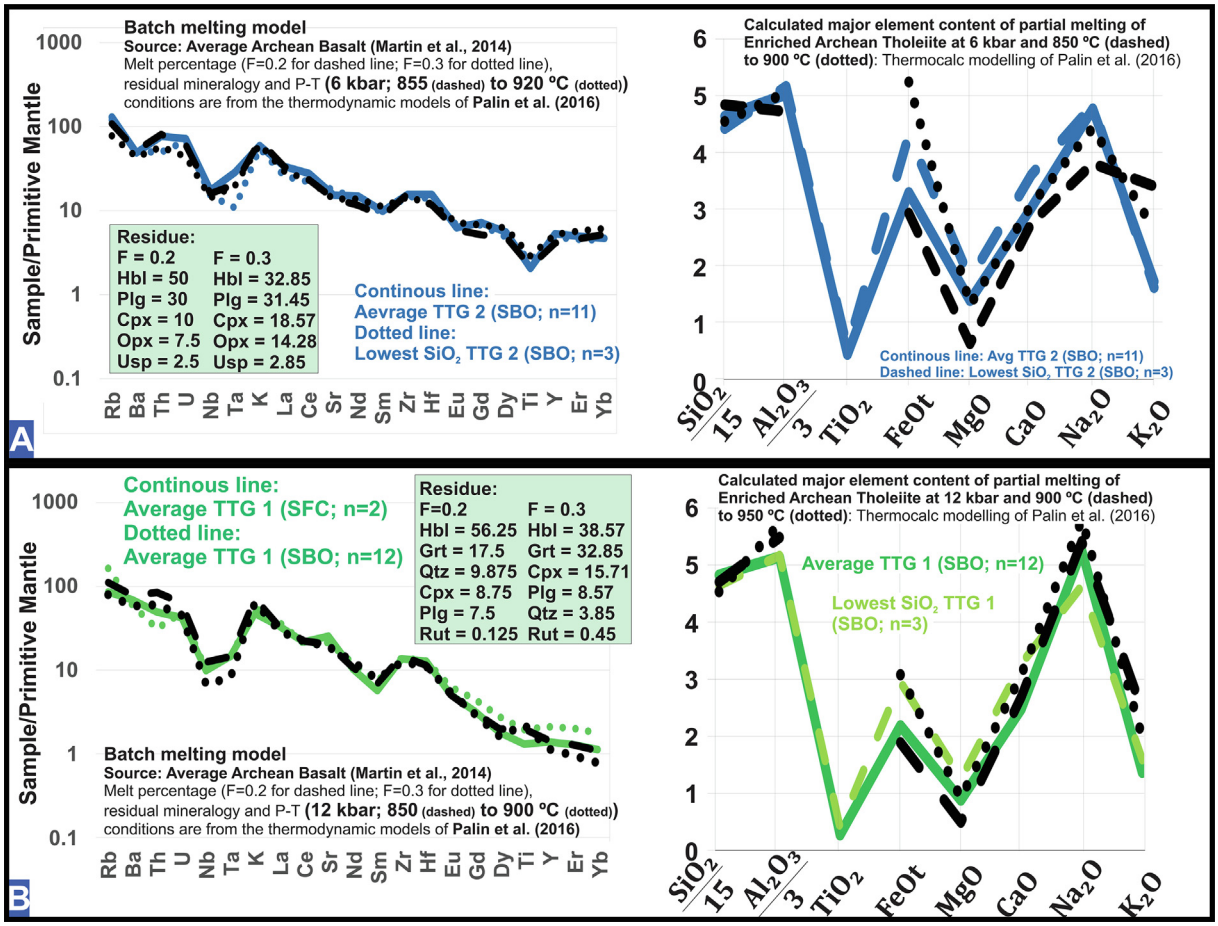

Fig. 9. Batch melting calculations, with variable restite modal compositions, using the average Archean basalt (Martin et al., 2014) as source. Primitive mantle is from McDonough and Sun (1995). Residual mineralogy, partial melt fraction and P–T conditions are from Palin et al. (2016). Partition coefficients are in Supplementary Material 5.

Moyen and Martin, 2012), the effects of water oversaturation (i.e., excess fluids) have recently been investigated (e.g., Pourteau et al., 2020; Hernández-Montenegro et al., 2021). Several studies, based on thermodynamic modelling using Thermocalc (Palin et al., 2016; Pourteau et al., 2020; Hernández-Montenegro et al., 2021), indicate the addition of excess water into a mafic source, at constant pressure, increases the amount of residual amphibole, decreases that of plagioclase, and has little effect in the stability of garnet. A TTG melt in equilibrium with such a residue would have higher La/Yb and Sr compared with a TTG in equilibrium with a residue lacking free-water (i.e., minimum saturation), but at similar pressures and temperatures (Pourteau et al., 2020; Hernández-Montenegro et al., 2021). This observation prompted Pourteau et al. (2020) to conclude that TTG previously considered as "high-pressure" (e.g., Moyen, 2011), could instead result from water-fluxed partial melting at lower pressures and shallower crustal levels (i.e., 9 kbar). Although an increase in both pressure and water contents during partial melting can result in a reduction in residual plagioclase (Palin et al., 2016; Pourteau et al., 2020), a pressure increase at constant temperature and constant minimum water saturation, will increase the amount of residual garnet and reduce the proportion of amphibole (Palin et al., 2016).

Although residual amphibole and garnet both increase the La/Yb ratio of the melt, Davidson et al. (2013) demonstrated that restitic amphibole decreases the Dy/Yb of the melt whereas garnet strongly increases it. Therefore, a plot of Sr/Zr versus Dy/Yb (Fig. 10) highlights differences in the composition of TTG melts brought about by: (a) increasing pressure; (b) higher free water contents in the mafic source or fractionation and/or solid–liquid unmixing involving plagioclase, amphibole (e.g., Laurent et al., 2020). In Fig. 10, there is a continuous trend from high-HREE, low-Sr TTG (i.e., TTG 2) towards low-HREE, high-Sr TTG (i.e., TTG 1), which seems to occur in other Archean terranes (e.g., Moyen, 2011). If the Dy/Yb ratio increases from low-Sr/Zr TTG (TTG 2) towards high-Sr/Zr TTG (TTG 1), it suggests that the content of residual garnet increased concomitant with the break-down of restitic plagioclase, which is expected for partial melting at progressively higher pressures (Palin et al., 2016). On the other hand, if increases in Sr/Zr were accompanied by decreasing Dy/Yb ratios this would suggest that residual garnet was either reduced or stayed unchanged, whereas the amount of amphibole increased, and plagioclase was totally or partially consumed. Such a trend is therefore consistent with fluid-fluxed partial melting (Pourteau et al., 2020). A similar trend would emerge from amphibole fractionation (decrease in Dy/Yb) and plagioclase accumulation, which would increase Sr contents (e.g., Laurent et al., 2020).

To evaluate these interpretations, the trace element contents of published TTG models are plotted in Fig. 10. The residual mineralogies calculated by Palin et al. (2016) at different pressures (6, 12 and 20 kbar) were used to perform batch-melting calculations and the results form a similar trend to that of our natural TTG, i.e., of increasing Sr/Zr with increasing Dy/Yb ratios (Fig. 10). In contrast, the trend formed by the modeled TTG of Pourteau et al. (2020), at constant pressure but increasing H_2O wt.%, is markedly different and defines a trend broadly perpendicular to that of the considered TTG.

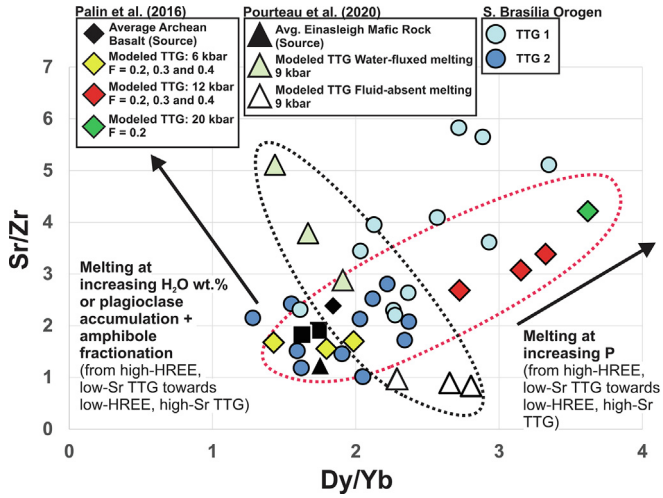

Fig. 10. Sr/Zr versus Dy/Yb diagram. Results of batch-melting calculations (average Archean basalt of Martin et al. 2014 as source) at different P–T conditions constrained by the thermodynamic modelling of Palin et al. (2016) are compared to the modelled TTG from Pourteau et al. (2020) and to TTG from the Southern Brasília Orogen. Black squares represent the average composition of the greenstone belts from the Southern São Francisco Craton.

Recently some authors have proposed that the high Sr and La/Yb contents of some TTG are related to plagioclase accumulation and amphibole fractionation, without the need for residual garnet (e.g., Laurent et al., 2020; Kendrick et al., 2022). However, these models fail to account for the increase in Dy/Yb and Sr/Zr in the TTG discussed here and will be not considered further.

In summary, the geochemical diversity of the TTG from the Southern Brasília Orogen has been modeled (batch melting) using a range of minor and trace elements attributed to pressure differences during partial melting. The thermocalc-constrained residual assemblages of Palin et al. (2016) at 6 and 12 kbar, and F values of 0.2 to 0.4, when applied to batch melting calculations yield trace element patterns similar to those of the studied TTG from SE Brazil (Fig. 9). In contrast, melts produced through water-fluxed melting (Pourteau et al., 2020), at a moderate pressure (9 kbar), are clearly distinct from that of the average TTG 1, with a concave-up HREE pattern (i.e., low Dy/Yb), and lower Sr and ∑REE contents, reflecting the larger amounts of residual amphibole (Pourteau et al., 2020).

TTG 2 melts segregated from their mafic parents at shallower levels (~6 kbar) and the TTG 1 melts were extracted from deeper segments within the crust (~12 kbar). A few rocks from the TTG 1 group could have been generated at even deeper levels and higher pressures, possibly in equilibrium with an eclogitic residue (Fig. 10), although more data is needed to evaluate that.

7.1.2. Granitoids and partial melting of TTG

Several studies point to the reworking of pre-existing continental crust, dominated by TTG, in the generation of granitic rocks in the Archean (e.g., Jayananda et al., 2006, 2020; Mikkola et al., 2012; Laurent et al., 2014a; Moyen et al., 2021). Partial melting of TTG produces rocks with high SiO_2 (70–75 wt.%), K_2O (2–6 wt.%) and $Al_2O_3/(FeO_t + MgO)$, similar to the analyzed biotite-two-mica granites (BTMG), transitional granitoids group 1 (TRAN.G1) and A-type granites group 1 (AGG1) (Fig. 8; Skjerlie and Johnston, 1992, 1993; Patiño Douce, 1997, 2005; Patiño Douce and McCarthy, 1998; Castro, 2004; Watkins et al., 2007). This indicates that these rocks could result from crustal melting of TTG, and this is consistent with the available geochronology, whole-rock Sm–Nd and zircon Lu–Hf data, as well as with field observations: (i) most of the BTMG, TRAN.G1 and AGG1 rocks are younger than the TTG; (ii) BTMG, TRAN.G1 and AGG1 samples have similar T_{DM} ages to the TTG, and they plot on similar $^{176}Hf/^{177}Hf$ crustal evolution trends (Fig. 6; Supplementary Materials 2 and 3), with the exception of two high-K samples from the Southern São Francisco Craton which have older T_{DM} ages than the analyzed TTG from the same region (Fig. 6), indicating their source could be older TTG, such as those from the Santa Bárbara Complex dated at ~3.2 Ga (e.g., Lana et al., 2013); and (iii) BTMG, TRAN.G1 and AGG1 rocks were emplaced during a period of high-grade regional metamorphism (~2.8–2.70 Ga) in the Southern São Francisco Craton (e.g., Lana et al., 2013; Farina et al., 2015; Albert et al., 2016; Cutts et al., 2019) and the Southern Brasília Orogen (this study).

Mildly peraluminous biotite granites, which comprise most of the samples analyzed, indicate an igneous source (Mikkola et al., 2012), although Laurent et al. (2014a) (and references therein) have highlighted that peraluminous granites (A/CNK >1.1) typically contain contributions from metasedimentary sources, as do S-type granites. In the Southern Brasília Orogen, only two BTMG samples have an A/CNK value >1.1, and in the Southern São Francisco Craton, only one such sample has been reported. Thus, we will not address this issue further. It is important to note that the TTG mapped in the Southern Brasília Orogen are migmatitic (metatexites and diatexites), have high-K thick leucossomes in some locations (Supplementary Material 2, Fig. S9), and are spatially associated with granite bodies, which indicates TTG have partially melted sometime during their history and likely generated the associated biotite granites.

Batch melting calculations, with residual mineralogy and melt fraction constrained by partial melting experiments of TTG (Skjerlie and Johnston, 1993; Watkins et al., 2007), as well as major element content comparisons of the analyzed high-K samples with glass compositions from experiments, indicate that TTG from the Southern Brasília Orogen and Southern São Francisco Craton are potential sources to the BTMG, TRAN.G1 and AGG1 rocks (Fig. 11). The compositional diversity of the granitoids derived from a TTG source can be explained by: (i) distinct source compositions, i.e. whether TTG 1 or TTG 2; (ii) degrees of partial melting, which varied from 25% to 42 %, at distinct P-T conditions; and (iii) the mineral assemblage of the residue.

Due to their low contents of $FeO_t + MgO + MnO + TiO_2$, CaO and HREE, biotite- two-mica granites (BTMG) and transitional granites group 1 (TRAN.G1) are better reproduced by partial melting of TTG 1 (Fig. 11A and B). On the other hand, A-type granites group 1 (AGG1) are richer in $FeO_t + MgO + MnO + TiO_2$, CaO and REE than BTMG, and so are thought to have been sourced from TTG 2 (Fig. 11C). In summary, many geochemical characteristics of melts are inherited from their source.

The degree of partial melting also influences the composition of the resulting melts. TRAN.G1 have elemental ratios (e.g., K_2O/Na_2O) and major element contents intermediate between those of TTG 1 and BTMG. The best fit with our batch melting calculations for TRAN.G1 was obtained with TTG 1 as the source (similar to starting material SC-5 of Watkins et al. (2007)), and a melt fraction (F) of 42% (7.6 kbar; 950 °C) obtained from fluid-absent run SC5-7 of Watkins et al. (2007) (Fig. 11). Although BTMG and TRAN.G1 likely share a similar source (i.e., TTG 1), the degree of melting (F) is larger for TRAN.G1 compared to BTMG samples (42% vs 25%), as is the temperature of melting (875 vs 950 °C) (Fig. 11A and B). In addition, differences in accessory minerals in the residual assemblage could explain some characteristics of TRAN.G1 and BTMG rocks. For instance, the presence of residual allanite, in addition to the major mineral composition of the residue established by experimental petrology (Watkins et al., 2007), might explain why TRAN.G1 have lower LREE, La/Yb and Th/U compared to their preferred source (i.e., TTG 1) and to BTMG, the latter modelled without residual allanite (e.g., Hermann, 2002).

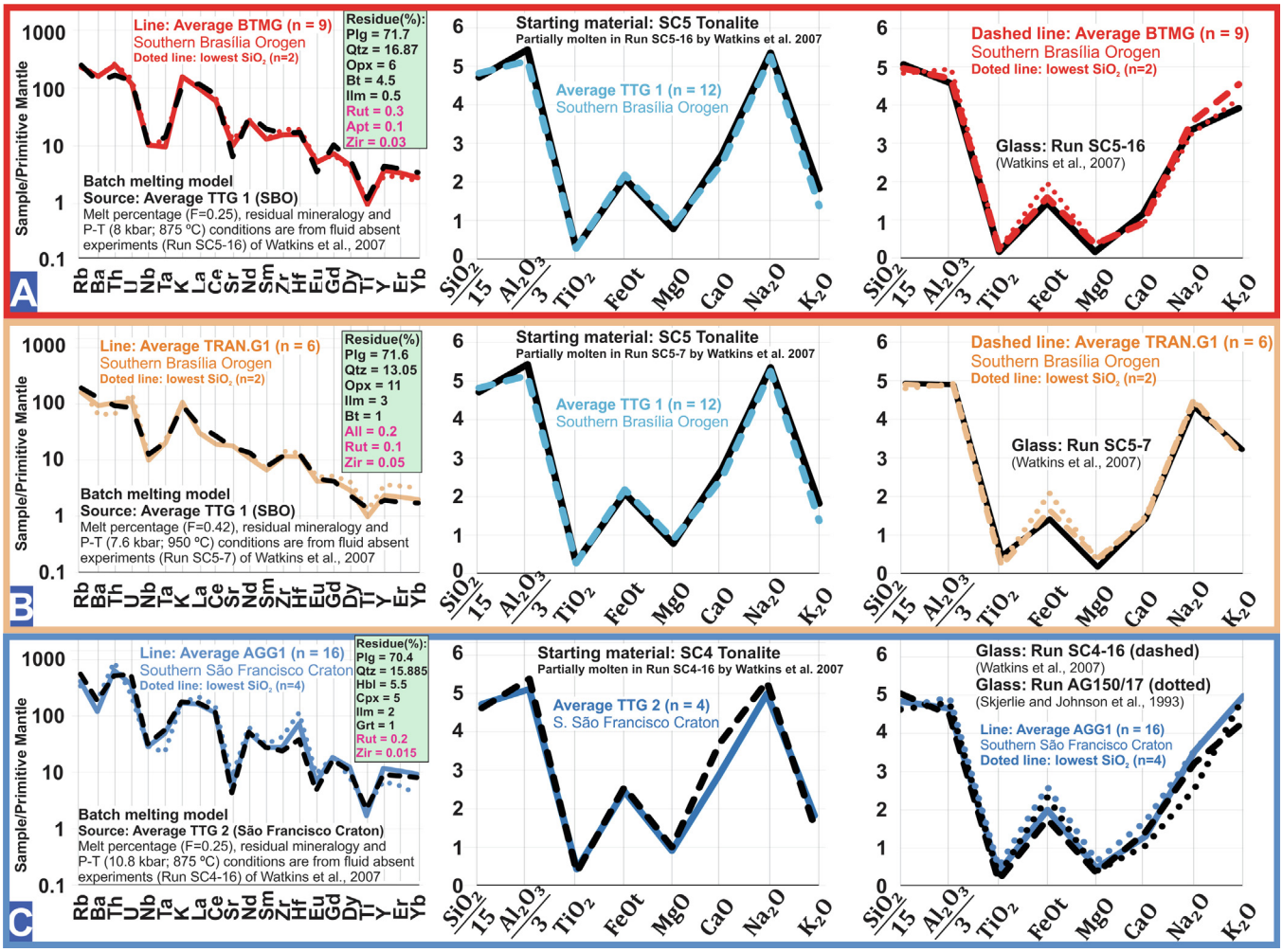

Fig. 11. Batch melting calculations, with variable restite modal compositions, using the TTG as source. Primitive mantle is from McDonough and Sun (1995). Residual mineralogy, partial melt fraction and P–T conditions are from Watkins et al. (2007). Samples from the Southern São Franscico Craton are from Farina et al. (2015) and Moreno et al. (2017). Partition coefficients are in Supplementary Material 5. Accessory residual minerals written in purple letters were not constrained by the experiments and are arbitrarily set, but were nevertheless observed during thin section analyses of the proposed sources.

Transitional granitoids group 1 (TRAN.G1) rocks have been interpreted as mixtures between a TTG melt and partial melts derived from anatexis of older continental crust (i.e., mostly TTG), as proposed by Farina et al. (2015) for the Southern São Francisco Craton. However, TRAN.G1 have lower Th and ∑REE contents than those that result from mixing TTG 1 and BTMG, and they can be more readily reproduced by batch melting calculations of a TTG 1 source (Fig. 11B). In addition, magma mixing textures have not been recognized for TRAN.G1 rocks in the Southern Brasília Orogen and we prefer models involving partial melting of TTG 1.

A-type granites group 1 (AGG1), which have only been recognized so far in the Southern São Francisco Craton (e.g., Moreno et al., 2017), have elevated HREE and HFSE, and these are not readily generated from TTG 1 (Supplementary Material 2, Fig. S5). AGG1 are also richer in FeO_t + MgO than the products of TTG 1 partial melting (i.e., BTMG and TRAN.G1). Still, AGG1 are mineralogically similar to BTMG, with K-feldspar, plagioclase, quartz and biotite as dominant phases (Bom Sucesso and Rio do Amparo granites of Moreno et al., 2017). This mineralogy indicates the AGG1 may be a product of TTG partial melting. Considering the average TTG 2 of the Southern São Francisco Craton as source, the trace element composition of the average AGG1 was successfully reproduced through batch melting calculations using the residual mineralogy of run SC4-16 (fluid absent) of Watkins et al. (2007), performed at 10.8 kbar and 875 °C (Fig. 11C). However, the AGG1 samples with the lowest SiO_2 values have higher FeO_t + MgO contents than that of the glass of run SC4-16 (Watkins et al., 2007; Fig. 11). In the experiments of Skjerlie and Johnston (1993) the selected starting material (AG150) is a tonalite rich in ferromagnesian minerals and very similar in composition to the lowest SiO_2 TTG 2 sample (not shown). When partially melted, AG150 produces melts (e.g., run AG150/17) with a similar composition to the lowest SiO_2 AGG1 samples (Fig. 11C). This suggests differences in composition among AGG1 rocks may be related to compositional variations of TTG 2 source rocks. The fact that AGG1 rocks contain large amounts of inherited zircon grains that match the age of regional TTG further supports the preferred petrogenetic model (Moreno et al. 2017).

7.1.3. An enriched mafic source for transitional granitoids group 2 and A-type granites group 2

Transitional granitoids group 2 (TRAN.G2) are only found in the Southern São Francisco Craton, and they comprise granites and granodiorites with plagioclase, quartz, K-feldspar and biotite, as well as the Samambaia Pluton of hornblende-bearing granitoids (Farina et al., 2015 and references therein). TRAN.G2 samples are too enriched in FeO_t, MgO and CaO to be a product of TTG partial melting, since experimental partial melting of TTG, even at very

high melt proportions, generates melts with MgO and FeO_t contents considerably lower than those of TRAN.G2 samples (Skjerlie and Johnston, 1992, 1993; Patiño Douce, 1997, 2005; Castro, 2004; Watkins et al., 2007). Due to a considerable enrichment in incompatible trace elements (e.g., REE), TRAN.G2 could not be modelled by partial melting of low-K mafic rocks, such as those from greenstone belts, which were successfully used to model the TTG. Moreover, melts from partial melting experiments of low-K basalts fail to replicate the high K_2O contents of TRAN.G2, that are between 2.6 wt.% and 3.2 wt.% (e.g., Rapp et al., 1991; Beard et al., 1994; Wolf and Wyllie, 1994). Similarly, the thermodynamic modelling of Palin et al. (2016) indicates that it is difficult to replicate the major-element composition of TRAN.G2 by partially melting the average enriched Archean tholeiite, which is similar in composition to the mafic rocks of the greenstone belts of the São Francisco Craton.

We investigate the possibility of partial melting of high-K amphibolites, since most of the TRAN.G2 samples plot in the high-K amphibolite field in the source discriminating diagram of Fig. 8 (Laurent et al., 2014a). Comparing the major element contents of TRAN.G2 with those of melts from partial melting experiments of high-K amphibolites (Rapp et al., 1991, 1999; Sen and Dunn, 1994; Patiño Douce and Beard, 1995; Sisson et al., 2005; Ye et al., 2021), those from run 87S35A-17 from Sisson et al. (2005) best resembles the average composition of TRAN.G2 (Fig. 12A). Still, the melt from run 87S35A-17 (Sisson et al., 2005) has higher K_2O than TRAN.G2 (Fig. 12A), which suggests the source of TRAN.G2 is poorer in K_2O compared to the amphibolite used as source in the experiments of Sisson et al. (2005). We used the residual mineralogy obtained from run 87S35A-17 (7 kbar, 900 °C and 13% of melt) to perform batch melting calculations and there is a good match between the calculated model and the average TRAN.G2 (Fig. 12A). As no high-K Archean amphibolites (SiO_2 < 53 wt.%) have yet been found in the Southern São Francisco, we used a high-K basalt sample from the Andean central volcanic zone as source in our modeling (Fig. 12B), once no trace element data is available for the high-K amphibolite used as source by Sisson et al. (2005).

Archean sanukitoids *sensu stricto* (e.g., Heilimo et al., 2010) and TRAN.G2 share a similar source (e.g., Laurent et al., 2014a) of high-K amphibolites, but there are compositional differences between these groups. The average K_2O content, for rocks of similar SiO_2, is higher in the sanukitoids *sensu stricto* (Heilimo et al., 2010; Laurent et al., 2011; Ma et al., 2013). In addition, sanukitoids are richer in Ba and Sr, but poorer in Th, LREE, HREE, Nb, Ta, Zr and Hf compared to TRAN.G2. These differences may result from distinct source compositions and/or variations in residual mineralogy during partial melting (or fractional crystallization). TRAN.G2 rocks are similar to high-silica endmembers of basalt-andesite-dacite-rhyolite (BADR) suites from modern arc settings (e.g., Martin et al., 2009). Therefore, these rocks were either generated in arc settings or are the product of reworking of mafic-intermediate rocks previously originated in arc settings.

The A-type granites group 2 (AGG2) are relatively rare, but they are distinctive in that they have relatively high FeO_t + MgO + MnO + TiO_2 contents, only matched by TTG 2, and elevated Ba/Rb (Supplementary Material 2, Fig. S8). Common minerals that incorporate Rb, such as biotite and K-feldspar, have larger D values for Ba (Bachmann et al., 2005; Fedele et al., 2015; see Supplementary Material 5), and so their presence in the residue decreases Ba/Rb of the melt. These features preclude TTG as sources for AGG2. Mafic rocks of the greenstone belts from the Southern São Francisco Craton are too depleted in incompatible trace element contents (e.g., REE, Nb, Ta, Zr, Hf, etc) to be likely sources of AGG2.

Since the most primitive AGG2 plot in the field of high-K amphibolites in the source discriminating diagram of Fig. 8 (Laurent et al., 2014a), we compared the major element contents of AGG2 to those of melts from partial melting experiments of high-K amphibolites and run AD19-3-1596 of Sisson et al. (2005) provided the best match (Fig. 12B). Hence, we selected a mafic rock that is similar to the starting material of Sisson et al. (2005) from the literature to use as source for batch melting calculations. The chosen rocks is a parental (primitive) enriched mafic rock from the well-studied HBG (hornblende biotite granites) A-type suite from Norway (Vander Auwera et al., 2003), which is mineralogically and compositionally similar to AGG2. The trace element pattern that resulted from the batch melting calculation is very similar to that of AGG2, including those of lower silica content. The selected source for AGG2 is richer in K_2O and incompatible trace element contents than the source of TRAN.G2 rocks discussed in the previous paragraph.

Whereas the Norwegian rocks are modeled by magma differentiation of mantle derived magma (Vander Auwera et al., 2003), AGG2 granitoids might have resulted from either partial melting or differentiation of the enriched mafic precursor (Fig. 12B). Mafic magmas associated with A-type granitoids are reported for several locations worldwide (e.g., Frost and Frost, 1997, 2011; Vander Auwera et al., 2003; Laurent et al., 2014b; Marangoanha et al., 2019). Similarly, one relatively mafic rock (~56 wt.%) was found close to the AGG2 sample (CAR) of the Southern Brasília Orogen by Valeriano et al. (2022).

Finally, and perhaps unexpectedly, the isotopic Hf-Nd signatures of AGG2 fall in the crustal evolution trend of the regional TTGs (Fig. 6; Supplementary Material 2, Fig. S4). This is interpreted in terms of subduction of crustal derived material into the mantle source regions (see Laurent and Zeh, 2015 for a similar interpretation), resulting in enriched isotope signatures and elevated Ba/Rb. There are a number of examples of incompatible-element-enriched mafic rocks, such as the calculated source for AGG2 rocks, which are also characterized by negative $\varepsilon_{Hf}(t)$ and $\varepsilon_{Nd}(t)$ values (e.g., Couzinié et al., 2016).

7.2. Geodynamics

In this section geochronological, geochemical and isotopic data are combined to evaluate the Archean geodynamic evolution in the Southern Brasília Orogen and Southern São Francisco Craton, from ~3.1 Ga to 2.6 Ga.

7.2.1. The generation of TTG from 3.05–2.95 Ga (Southern Brasília Orogen) to ~2.90–2.77 Ga (Southern São Francisco Craton)

The TTG of the Southern São Francisco Craton have been modeled as partial melts of the average mafic magmatic rocks from adjacent Archean greenstone belts (Rio das Velhas and Pitangui). The greenstone belt rocks have immobile trace element compositions similar to those of basaltic rocks from modern island arc environments (compare green and red lines with dashed black line in Fig. 13A). They differ markedly from Cenozoic basaltic rocks of intra-plate settings, such as oceanic plateaus, continental flood basalts and oceanic islands (yellow field, Fig. 13A), and these differences are maintained when considering a broader spectrum of trace elements, including more mobile LILEs as well as HFSE (Fig. 13B). The younger rocks tend to have higher Sr and Ba contents than those in the Archaean (Fig. 13B), but both Archean and Quaternary suites have negative HFSE and Nb-Ta-Ti anomalies, and elevated Th/Nb (Fig. 13C and D). It could be argued that these features arise from minor crustal contamination (e.g., Moyen and Laurent, 2018). However, the trends observed in Fig. 11 are inconsistent with contamination with the average upper crust of the Southern São Francisco Craton (red arrow in Fig. 13) and consistent with fluid-fluxing of a (primitive) mantle source in a subduction

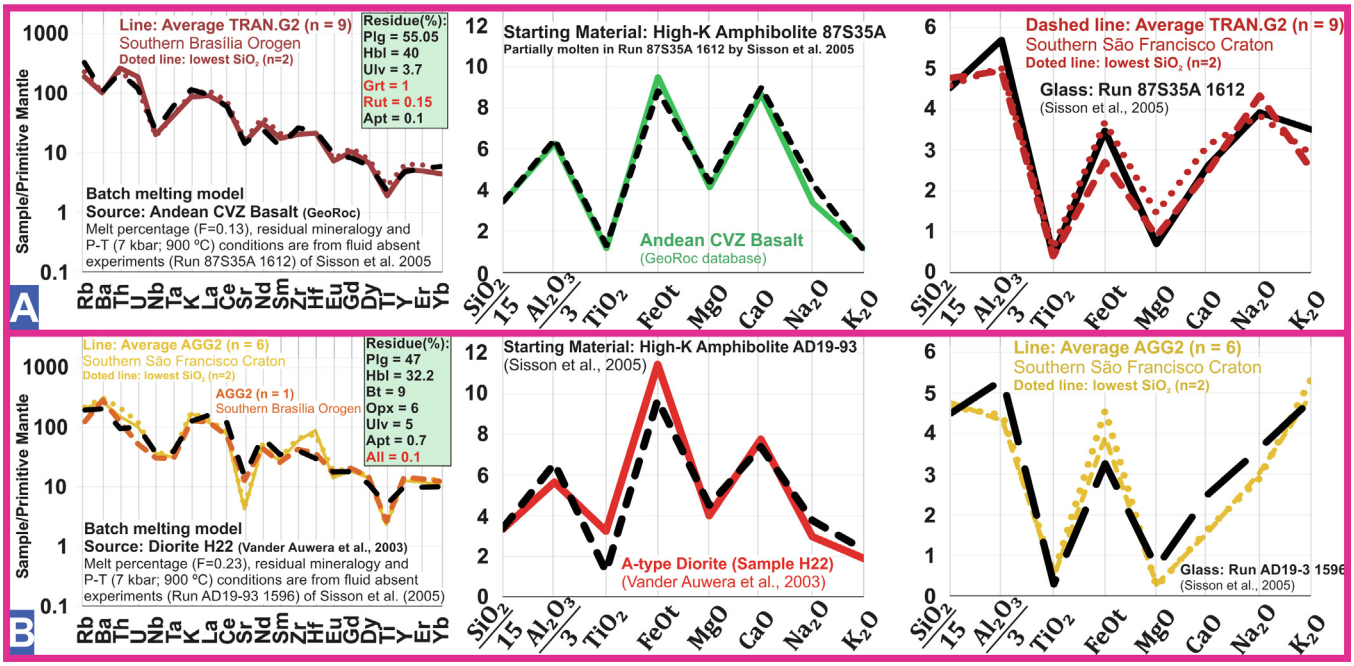

Fig. 12. Batch melting calculations, with variable restite modal compositions, using the high-K amphibolites as sources. Primitive mantle is from McDonough and Sun (1995). Residual mineralogy, partial melt fraction and P–T conditions are from Sisson et al. (2005). Samples from the Southern São Franscico Craton are from Farina et al. (2015) and Moreno et al. (2017). Partition coefficients are in Supplementary Material 5. Accessory residual minerals written in red letters were not constrained by the experiments and are arbitrarily set.

(or subduction-like, e.g., Bédard, 2018) environment (black arrow in Fig. 13).

The tectonic settings involved in the generation of crustal melts, such as TTG, remain difficult to constrain geochemically, since incompatible trace element ratios of silicic rocks may be inherited from their crustal source rocks (e.g., Moyen and Laurent, 2018). However, the TTG from the Southern São Francisco Craton are broadly coeval with their inferred source rocks, the mafic rocks from adjacent greenstone belts (Fig. 14), and so it appears that they are part of associated magmatic events, and as such share similar subduction-related tectonic settings. The TTG from the Southern Brasília Orogen (Amparo Complex, this study) are not spatially associated with large-scale greenstone belts and they could have been part of a distinct block before ~2.8–2.7 Ga (e.g., Cioffi et al., 2016a, 2016b). However, our modelling shows that rocks similar to those of the greenstone belts of the São Francisco Craton could have been the sources of the Amparo Complex TTG (Supplementary Material 2, Fig. S7).

The TTG from the São Francisco Craton (Albert et al., 2016) and the Southern Brasília Orogen have chondritic to more depleted, mantle-like initial Hf and Nd isotope ratios (Fig. 6), which is typical of TTG worldwide (e.g., Laurent et al., 2014a). We conclude that the TTG represent partial melting of juvenile continental crust, and the minor and trace elements indicate that these sources were generated in a subduction-related setting. The TTG sources are very similar to modern island arcs, and it is likely the TTG were generated during accretion of island arcs, causing partial melting of the crust at different depths, thus generating TTG 1 (12 kbar) at the base of thickened crust (~40 km in depth) and TTG 2 at shallower levels (6 kbar).

7.2.2. Medium and high-K granitoids (2.85–2.70 Ga): what drives extensive crustal reworking?

The period from 2.85 Ga to ~2.70 Ga, is characterized by an increased diversity of granitoids, typically with high K_2O and incompatible element contents. These rocks have been divided into different geochemical groups (BTMG, TRAN.G1, TRAN.G2 and AGG1) and many are thought to reflect partial melting of TTG, including A-types group 1, as evidenced by batch melting calculations (see Sections 6.1.2), geochronology and Hf-Nd isotopic signatures (Fig. 6; Supplementary Material 2, Figs. S3 and S4), or partial melting of arc-related high-K amphibolites (TRAN.G2). They were generated at a time of peak metamorphic activity in response to crustal thickening (Fig. 14, PDP at the top of the figure, Lana et al., 2013; Farina et al., 2015; Albert et al., 2016). Older ages of metamorphism at the time of peak TTG activity between 3.1 Ga and 2.8 Ga have been reported (e.g., Teixeira et al., 1998), but they are much less common.

The development of diverse granites/granitoids from partial melting of TTGs at ~2.8–2.7 Ga, marks a change in tectonic regime and an increase in the chemical maturity of the continental crust (e.g., increases in K_2O/Na_2O, Rb/Sr and Th/Nb with time in Fig. 7). Such K-rich granites are a feature of the stabilization of Archaean cratons (e.g., Laurent et al., 2014a), and in the Southern São Francisco they are co-incident with high- to medium grade regional metamorphism peaking at ~2.72 Ga (Fig. 14). Late Archaean metamorphic temperatures exceeded 700–900 °C (Teixeira et al., 1998; Lana et al., 2013; Farina et al., 2015; Albert et al., 2016; Cioffi et al., 2016a; Aguilar et al., 2017; Cutts et al., 2019; Brando-Soares et al., 2020; this study), and Archean amphibolites, gneisses and schists from the Southern São Francisco yielded peak conditions of 650 to 700 °C and 8 to 9 kbar, with a clockwise P–T path (Cutts et al., 2019). Such conditions are consistent with crustal thickening and they suggest that lithosphere stabilization was linked to lateral tectonics and accretion/continental collision (Albert et al., 2016).

Pervasive migmatization of TTG in the Southern Brasília Orogen (Supplementary Material 2, Fig. S9) highlights that these rocks melted at some point during their history, and the metamorphic ages obtained from two migmatitic TTG of ~3.00–2.95 Ga are 2.88 and 2.72 Ga, concomitant with the metamorphic peak for the Southern São Francisco Craton (Supplementary Material 2, Fig. S3G and I; Fig. 14). Therefore, it is likely that these ages repre-

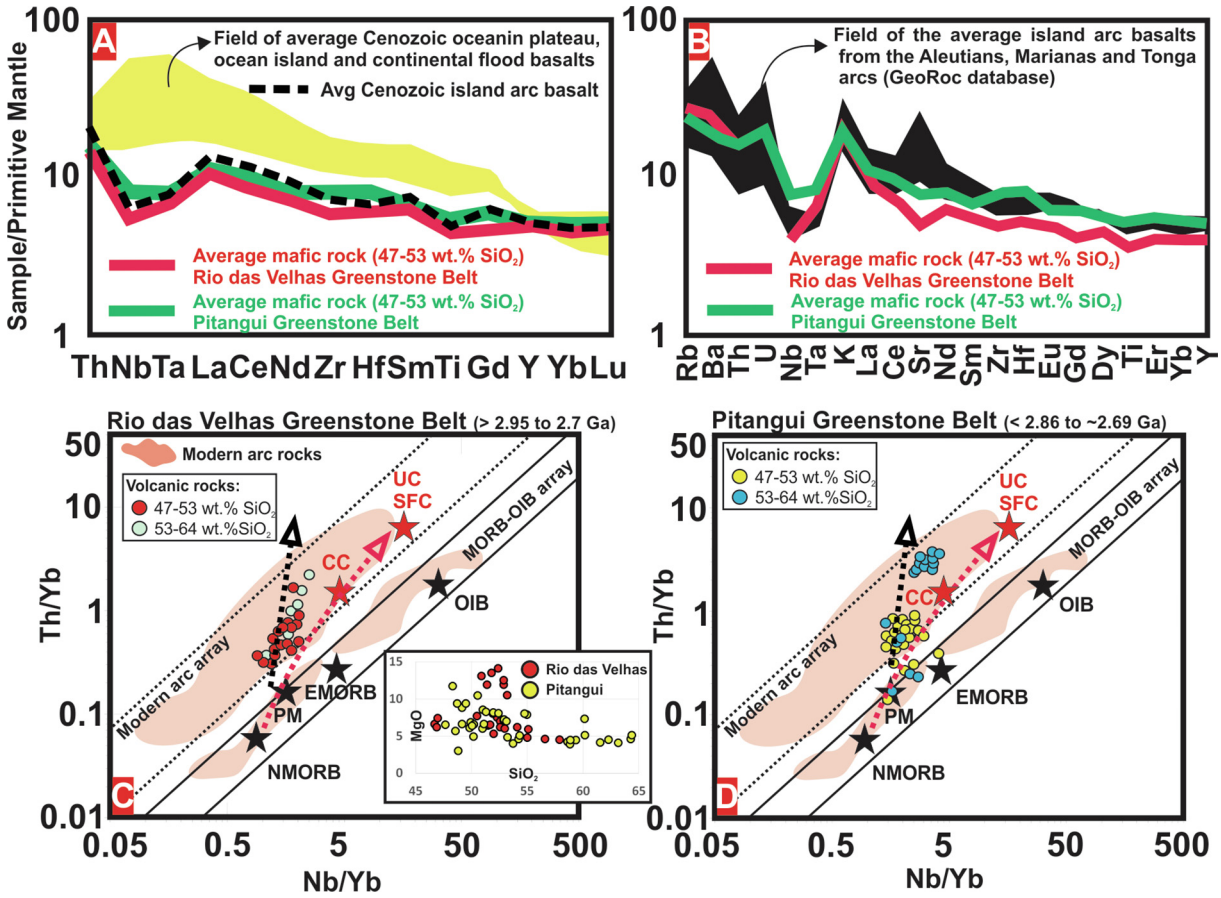

Fig. 13. (A and B) Primitive mantle (McDonough and Sun, 1995) normalized diagrams. (A) Metabasalts from different geotectonic settings (from Li et al., 2015) and from greenstone belts of the São Francisco Craton (Zucchetti et al., 2000; Verma et al., 2017; Brando-Soares et al., 2020). The Cenozoic island arc basaltic rocks are from the Aleutian, Kurile, Ryukyu, Lesser Antilles and Sunda arcs (Li et al., 2015). (B) the average composition of Quaternary island arc basalts from the Marianas, Aleutians and Tonga island arcs (GeoRoc database) are plotted together with the average basalts of the greenstone belts of the Southern São Francisco Craton. (C and D) Th/Yb versus Nb/Yb (Pearce, 2008) diagrams. Red field of modern arc rocks is from Moyen and Laurent (2018). Red arrow represents mixing of a basalt extracted from the mantle with the average continental crust and the average upper crust of the Southern São Francisco Craton (red stars). Black arrow represents enrichment by fluids in an arc environment. Both arrows are from Moyen and Laurent (2018).

sent a metamorphic event which caused migmatization and these ages are similar to the ages of biotite granites and other lithologies related to the partial melting of TTG. Migmatization and the development of K-rich crustal melts likely resulted from the amalgamation of exotic blocks to the nuclei of Southern São Francisco Craton, such as the Amparo Complex of the Southern Brasília Orogen (Cioffi et al., 2016a, 2016b), and the collision of the Belo Horizonte and Bonfim complexes with the Divinópolis Complex, as suggested by Brando-Soares et al. (2020).

7.2.3. A-type granites (AGG2) and crustal extension (2.70 to 2.6 Ga)

The youngest set of granites from the studied region are post-collisional A-type group 2 (e.g., Moreno et al., 2017). In some Archaean and younger orogens, the late- to post-collisional rocks are magnesium-potassic sanukitoids *sensu stricto* (e.g., Fowler and Rollinson, 2012; Laurent et al., 2014b), but they tend not to be restricted to the post-collisional stage and they commonly occur during preceding arc activity. The more primitive (46–52 wt.% SiO_2) ferroan A-types, such as those from Norway (e.g., Bogaerts et al., 2003; Vander Auwera et al., 2003), have higher FeO_t, TiO_2, HFSEs and lower contents of MgO than sanukitoids *sensu stricto* (e.g., Heilimo et al., 2010; Laurent et al., 2011). Otherwise, these two groups have many similarities. They both typically have expanded series from high-K mafic to felsic lithologies (e.g., Vander Auwera et al., 2003; Lobach-Zhuchenko et al., 2008), but the A-types have higher zircon saturation temperatures, which may be why they have higher TiO_2 (Sisson et al., 2005) and HFSE contents, and they are less hydrated (Eby, 1992; Frost and Frost, 1997, 2011; Dall'Agnol et al., 2005; Collins et al., 2020).

Fig. 15 discriminates between silicic magmas generated in continental collisions and magmatic arcs from those generated in intraplate settings, such as continental rifts or continental floods. The AGG2 from this study (yellow triangles and circle) are distinctive in that they plot in the rift and continental flood fields. They are therefore thought to be related to lithospheric extension (e.g., Albert et al., 2016), whereas other medium to high-K granitic rocks studied here (red triangles and circles) plot in a similar field to that of Himalayan leucogranites, Archean sanukitoids and Quaternary Andean CVZ rocks (Fig. 15).

The AGG2 rocks, emplaced between ~2.7 Ga and ~2.6 Ga, are geographically associated with (Fig. 1) and closely followed in time by the emplacement of dyke swarms at ~2.55 Ga, which provide strong evidence of crustal extension, and lithospheric stabilization in that the lithosphere had sufficient rigidity to fracture (Caxito et al., 2020). Mafic dykes represent the last period of Archean magmatic activity in the region. Localized partial melting of crustal lithologies (e.g., TTGs and/or metasedimentary rocks), concomitant with extension and mantle-derived magmatism, also occurred in the Southern São Francisco Craton (e.g., Simon et al., 2018).

The AGG2 rocks have been modeled as partial melts or differentiates of mafic rocks and their calculated source rocks have higher incompatible elements than MORB or the inferred source rocks of

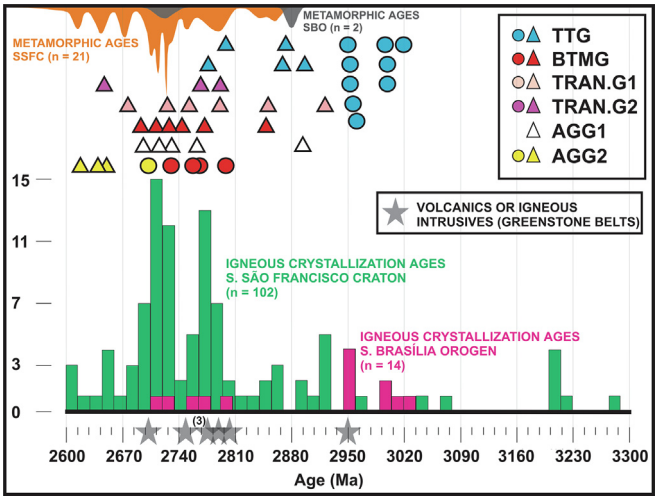

Fig. 14. Bottom green and pink histograms represent the available U–Pb age data for granitoids (Supplementary Material 4) in the studied regions, including those for which geochemistry data is not available. Granitoid samples from the São Francisco Craton (triangles; Farina et al., 2015; Albert et al., 2016; Moreno et al., 2017) and the Southern Brasília Orogen (circles; Cioffi et al., 2016a; this study), for which both geochemistry and high-quality igneous crystallization U–Pb ages are available, are plotted (triangles and spheres) directly above their respective crystallization ages (*x* axis). Gray stars represent mafic to felsic volcanics and intrusives from the greenstone belts, for which there are reliable U–Pb data (e.g., Moreira et al., 2019). The orange probability density plot at the top of the figure summarises U–Pb zircon (overgrowth, soccer-ball grains, etc.) and monazite metamorphic ages obtained from the southern São Francisco Craton (n = 19; the reader is referred to Supplementary Material 4 for references) and the grey probability density plot summarises Archean metamorphic ages from the Southern Brasília Orogen (this study).

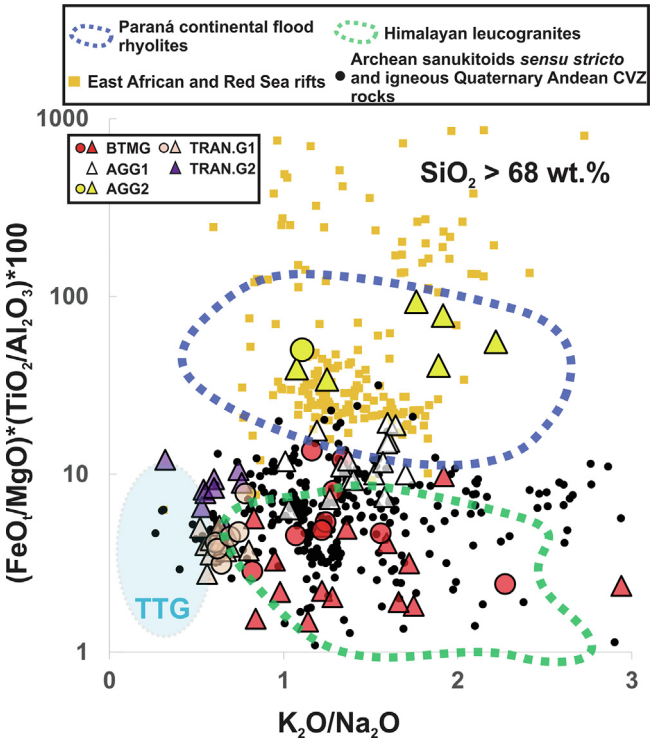

Fig. 15. $(FeO_t/MgO)^*(TiO_2/Al_2O_3)^*100$ vs K_2O/Na_2O diagram. Samples from the Southern São Francisco Craton are from Farina et al. (2015) and Moreno et al. (2017) and are represented by triangles, whereas circles represent samples from the Southern Brasília Orogen (Cioffi et al., 2016a; this study). Archean sanukitoid samples are from Heilimo et al. (2010), Laurent et al. (2011) and Ma et al. (2013). Samples from the Andean CVZ, East African and Red Sea rifts and Paraná continental flood are from the GeoRoc database (http://georoc.mpch-mainz.gwdg.de/georoc/). Himalayan leucogranites are from Guo and Wilson (2012).

the TTG (Fig. 12B). The overall trace-element pattern of the calculated source of AGG2 rocks is similar to that of modern arc-related basalts (GeoRoc database), as are their Th/Nb ratios (0.2–0.8). Thus, late magmatism in the Southern São Francisco Craton tapped a mantle source apparently metasomatized by subduction activity, which led to enrichment of incompatible elements, and radiogenic isotope ratios. Mantle enrichment has been commonly associated with subduction zone activity in the generation of sanukitoids *sensu lato* in the Archean (e.g., Heilimo et al., 2010, 2013; Laurent et al., 2014a), and it is consistent with the preferred model for TTG generation associated with subduction in the Mesoarchean, illustrated by basement rocks of the Southern Brasília Orogen (see Section 6.2.1).

7.3. Comparisons to other cratons

Many Archean domains worldwide broadly exhibit a magmatic evolution similar to that of the Southern São Francisco Craton, with a period of dominantly juvenile TTG magmatic activity followed by magmatic diversification and emplacement of biotite- two-mica granites, sanukitoids, A-types, transitional and hybrid granitoids (e.g., Laurent et al., 2014a and references therein). Late Archean granitoid diversification, however, occurred at different times in different Cratons and lasted for different time spans (Laurent et al., 2014a; Supplementary Material 2, Fig. S10). Moreover, unlike the largely juvenile TTG activity, late Archean magmatism is characterized by varying $\varepsilon_{Hf}(t)/\varepsilon_{Nd}(t)$ signatures concomitant with both new crustal additions and reworking (Laurent et al., 2014a). In the Southern São Francisco Craton, reworking dominated in the generation of K-rich granites, and it was then following by extension and extension related magmatism (e.g., Albert et al., 2016; Fig. 16).

The crustal isotopic evolution for the Southern São Francisco is similar to that for the Pietersburg block (Kaapvaal Craton), for example, with juvenile TTG activity between ~3.3–3.2 Ga and 2.95 Ga, followed by high K_2O/Na_2O magmatism and crustal reworking (e.g., Laurent et al., 2014a and references therein; Zeh et al., 2013; Albert et al., 2016; this study). In both terrains greenstone belt magmatism is roughly coeval with TTG emplacement (e.g., Laurent et al., 2014a, 2014b and references therein), and the timing and duration of high K_2O/Na_2O late-stage Neoarchean magmatism is also similar (Fig. 17). It starts at approximately 2.8 Ga and lasts for approximately 200 Myr (this study; Laurent et al., 2014a), and relatively large volumes of anatectic granitoids, and hybrids prevailed between 2.8 Ga and ~2.7 Ga in both cratons (Laurent et al., 2014a). They have been modeled as crustal melts of previously emplaced TTG (this study) during crustal thickening and continental collision (Laurent et al., 2014b and references therein; Farina et al., 2015). This lasted until the late stages of Archean magmatic activity, and from ~2.7 Ga to ~2.6 Ga considerably lower volumes of A-types (and hybrids) were emplaced, such as the Matok Pluton in the Pietersburg block (Laurent et al., 2014a, 2014b), in response to post-collisional orogenic collapse in an extensional regime (Fig. 17; this study; Laurent et al., 2014a).

The timing of onset of Archean high-K magmatism occurred at different times in different Cratons (Laurent et al., 2014a; Cawood et al., 2018). This is illustrated by the example of the Pilbara Craton (Hickman, 2012; Hawkesworth and Kemp, 2021), where high-K magmatism started at ~3.0 Ga, approximately 200 Myr earlier than in the Southern São Francisco Craton (Supplementary Material 2, Fig. S11). Interestingly the development of elevated K_2O/Na_2O in the Pilbara rocks appears to be associated with more rocks with high $(FeO_t/MgO)^*(TiO_2/Al_2O_3)^*100$ values, indicating a greater contribution from intraplate magmas associated with cra-

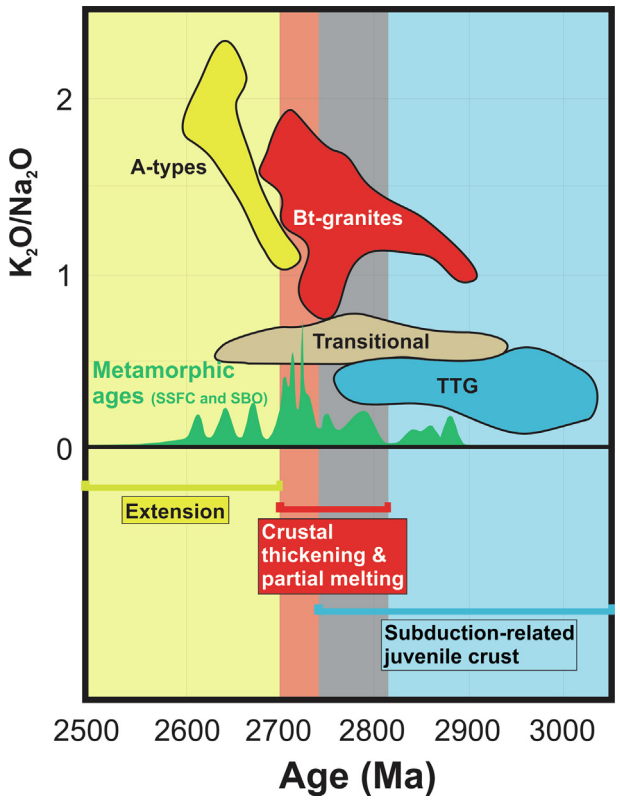

Fig. 16. Summary diagram, showing important granitoid groups from the Southern São Francisco Craton (Farina et al., 2015; Moreno et al., 2017) and Southern Brasília Orogen (Cioffi et al., 2016a; this study). This is a tectonic evolution similar to that proposed by Albert et al. (2016) and references therein.

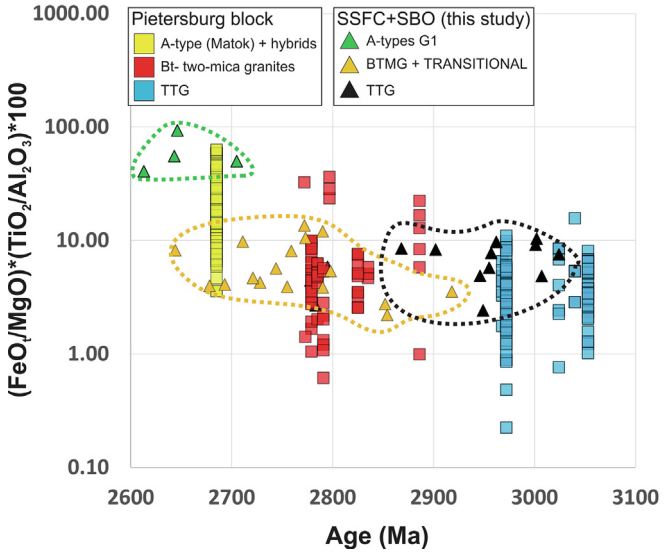

Fig. 17. Diagram of $(FeO_t/MgO)*(TiO_2/Al_2O_3)*100$ versus age, and the data in Fig. 15 indicate that rocks with $(FeO_t/MgO)*(TiO_2/Al_2O_3)*100$ higher than ~20 have a significant intraplate component. Samples from the Southern São Francisco Craton (SSFC) and Southern Brasília Orogen (SBO) are shown as triangles (Farina et al., 2015; Cioffi et al., 2016a; Moreno et al., 2017; this study). Samples from the Pietersburg block of the Kaapvaal Craton, South Africa, are shown as squares (Laurent et al., 2019 and references therein).

ton stabilization (Supplementary Material 2, Fig. S11). Extensional A-types may have been emplaced late in the evolution of cratons in response to orogenic collapse and drier conditions related to the cessation of subduction activity following continental collision. Subduction can efficiently transport water from the surface to the mantle and thus hinder the production of anhydrous magmas, such as A-types (e.g., Frost and Frost, 2011).

The period ~2.9–2.5 Ga marks the onset of prolific crustal reworking and the stabilization of Archaean cratons globally (e.g., Condie and Aster, 2010; Laurent et al., 2014a; Cawood et al., 2018; Moyen and Laurent, 2018), and a similar record is preserved in the Southern São Francisco Archaean rocks. It is possible that this period represents the sequential amalgamation of continental blocks that ultimately formed an Archean supercontinent (e.g., Hawkesworth et al., 2013 and references therein), albeit the occurrence of an early manifestation of the Wilson cycle is still debated.

8. Concluding remarks

Three major periods of granitoid production have been identified in the Archean terranes of the Southern Brasília Orogen and the Southern São Francisco Craton (Fig. 14). They range in age from 3.05 Ga to 2.60 Ga, and each period reflects a distinct tectonic mode in the evolution of this segment of Archean crust. They can be summarized as follows:

(1) Juvenile TTG magmatism, closely associated with subduction related magmatism preserved in adjacent greenstone belts (e.g., Moreira et al., 2019; Brando-Soares et al., 2020), occurred from ~3.05 Ga to 2.80 Ga. The TTG were subdivided into TTG 1, with high Sr and low HREE, and TTG 2, with low Sr and high HREE. The trend formed by TTG 1 and 2 in a Sr/Zr versus Dy/Yb diagram is used to discriminate between TTG generated by fluid fluxing at moderate crustal levels (e.g., Pourteau et al., 2020) or amphibole fractionation with plagioclase accumulation (e.g., Laurent et al., 2020) from those generated by partial melting at different pressures (e.g., Palin et al., 2016). The trend of the studied TTG from SE Brazil is consistent with partial melting of average greenstone belt basalts over a range of pressures from ~12 kbar for TTG 1 to ~6 kbar for TTG 2. TTG are broadly coeval with greenstone belt volcanics of the Southern São Francisco Craton, and those of mafic composition, and the inferred sources of the TTG, have elevated Th/Nb indicating formation in a subduction setting (e.g., Brando-Soares et al., 2020). Accretion of island-arcs may have led to the partial melting of metabasalts at different pressure conditions.

(2) Reworking of pre-existing TTG is the dominant mode of magmatic activity from ~2.85 Ga to 2.70 Ga. This leads to the generation of relatively large amounts of granite, including A-type rocks (AGG1) and biotite- two-mica granites, and the diversity within these K-rich granites is attributed to: (i) differences in source composition, whether TTG 1 or TTG 2; (ii) distinct melt fractions (F), from 18% to 40%; and (iii) the residual phases stable during partial melting. The reported P–T conditions of 8–9 kbar and 650 to 800 °C in the late Archaean (e.g., Cutts et al., 2019), concomitant with crustal reworking, is consistent with crustal thickening associated with accretion/continental collision (Albert et al., 2016).

(3) Post-collisional extension occurred between 2.70 Ga and 2.55 Ga, evidenced by mafic dyke swarms enriched in incompatible elements (e.g., Caxito et al., 2020) and A-types group 2 granites (Farina et al., 2015; this study). These A-types have Ba/Rb and $FeO_t + MgO + TiO_2 + MnO$ contents that are too high to have been generated by partial melting of exposed crustal rocks from the Southern São Francisco Craton. Extensional A-type granites (AGG2) appear to have been related to magmas derived from subduction-

metasomatized subcontinental mantle, followed by differentiation or partial melting to generate the evolved granites. Extension-related granitic A-types can be discriminated from crustal partial melts and subduction-related magmas through a $(FeO_t/MgO)^*(TiO_2/Al_2O_3)^*100$ versus K_2O/Na_2O diagram. The development of intraplate, extensional granites strikingly marks the end of Archaean magmatism, and, although it is volumetrically limited, it is attributed to collapse of tectonically thickened crust associated with the cessation of subduction and collisional activity and the stabilization of lithosphere in the Southern São Francisco and other cratons.

The rocks in the Archean of the Southern Brasília Orogen and the Southern São Francisco Craton are >3.05 Ga in age, and their geological evolution is consistent with the occurrence of plate tectonics at that time, broadly similar to processes active at the present day.

Declaration of Competing Interest

The authors declare that they have no known competing financial interests or personal relationships that could have appeared to influence the work reported in this paper.

Acknowledgements

Rodrigo Schwantes Marimon is thankful to Fundação Carlos Chagas de Amparo à Pesquisa do Estado do Rio de Janeiro (FAPERJ), for providing him a post-doctoral fellowship (E-26/202.084/2020 and 2020.03701.1). R.A.J. Trouw acknowledges the National Council for Scientific Development (CNPq) for financial support. Everton M. Bongiolo acknowledges CNPq for his Productivity on Research grant (# 311106/2020-0). Careful editorial handling by M. Santosh and excellent suggestions, which considerably improved the quality of the manuscript, made by Oscar Laurent, Richard Palin and an anonymous reviewer are greatly acknowledged.

Appendix A. Supplementary data

Supplementary data to this article can be found online at https://doi.org/10.1016/j.gsf.2022.101402.

References

Aguilar, C., Alkmim, F.F., Lana, C., Farina, F., 2017. Palaeoproterozoic assembly of the São Francisco craton, SE Brazil: New insights from U-Pb titanite and monazite dating. Precambrian Res. 289, 95–115.

Albert, C., Farina, F., Lana, C., Stevens, G., Storey, C., Gerdes, A., Dopico, C.M., 2016. Archean crustal evolution in the Southern São Francisco craton, Brazil: Constraints from U-Pb, Lu-Hf and O isotope analyses. Lithos 266, 64–86.

Alkmim, F.F., Marshak, S., 1998. Transamazonian orogeny in the Southern Sao Francisco craton region, Minas Gerais, Brazil: evidence for Paleoproterozoic collision and collapse in the Quadrilátero Ferrıfero. Precambrian Res. 90 (1–2), 29–58.

Ávila, C.A., Teixeira, W., Cordani, U.G., Moura, C.A.V., Pereira, R.M., 2010. Rhyacian (2.23–2.20 Ga) juvenile accretion in the southern São Francisco craton, Brazil: Geochemical and isotopic evidence from the Serrinha magmatic suite, Mineiro belt. J. S. Am. Earth. Sci. 29 (2), 464–482.

Ávila, C.A., Teixeira, W., Bongiolo, E.M., Dussin, I.A., Vieira, T.A.T., 2014. Rhyacian evolution of subvolcanic and metasedimentary rocks of the southern segment of the Mineiro Belt, São Francisco Craton, Brazil. Precambrian Res. 243, 221–251.

Bachmann, O., Dungan, M.A., Bussy, F., 2005. Insights into shallow magmatic processes in large silicic magma bodies: the trace element record in the Fish Canyon magma body, Colorado. Contrib. Mineral. Petrol. 149 (3), 338–349.

Baltazar, O.F., Zucchetti, M., 2007. Lithofacies associations and structural evolution of the Archean Rio das Velhas greenstone belt, Quadrilátero Ferrífero, Brazil: A review of the setting of gold deposits. Ore Geol. Rev. 32 (3–4), 471–499.

Barbosa, N.S., Teixeira, W., Ávila, C.A., Montecinos, P.M., Bongiolo, E.M., 2015. 2.17–2.09 Ga crust forming episodes in the Mineiro belt, São Francisco craton, Brazil: U-Pb ages and geochemical constraints. Precambrian Res. 270, 204–225.

Beard, J.S., Lofgren, G.E., 1991. Dehydration melting and water-saturated melting of basaltic and andesitic greenstones and amphibolites at 1, 3, and 6.9 kb. J. Petrol. 32 (2), 365–401.

Beard, J.S., Lofgren, G.E., Sinha, A.K., Tollo, R.P., 1994. Partial melting of apatite-bearing charnockite, granulite, and diorite: Melt compositions, restite mineralogy, and petrologic implications. J. Geophys. Res.-Solid Earth 99 (B11), 21591–21603.

Bédard, J.H., 2018. Stagnant lids and mantle overturns: Implications for Archaean tectonics, magmagenesis, crustal growth, mantle evolution, and the start of plate tectonics. Geosci. Front. 9 (1), 19–49.

Bogaerts, M., Scaillet, B., Liégeois, J.P., Vander Auwera, J., 2003. Petrology and geochemistry of the Lyngdal granodiorite (Southern Norway) and the role of fractional crystallisation in the genesis of Proterozoic ferro-potassic A-type granites. Precambrian Res. 124 (2–4), 149–184.

Brown, M., Johnson, T., Gardiner, N.J., 2020. Plate tectonics and the Archean Earth. Annu. Rev. Earth Planet. Sci. 48, 291–320.

Campos, J., Carneiro, M.A., Basei, M.A., 2003. U-Pb evidence for late Neoarchean crustal reworking in the southern São Francisco cráton (Minas Gerais, Brazil). Anais da Academia Brasileira de Ciências 75 (4), 497–511.

Campos Neto, M.C., Basei, M.A.S., Janasi, V.A., Moraes, R., 2011. Orogen migration and tectonic setting of the Andrelândia Nappe system: An Ediacaran western Gondwana collage, south of São Francisco craton. J. S. Am. Earth. Sci. 32 (4), 393–406.

Castro, A., 2004. The source of granites: inferences from the Lewisian complex. Scot. J. Geol. 40 (1), 49–65.

Cawood, P.A., Hawkesworth, C.J., Pisarevsky, S.A., Dhuime, B., Capitanio, F.A., Nebel, O., 2018. Geological archive of the onset of plate tectonics. Phil. Trans. R. Soc. London 376, 20170405.

Caxito, F.A., Hagemann, S., Dias, T.G., Barrote, V., Dantas, E.L., Chaves, A.O., Campello, M.S., Campos, F.C., 2020. A magmatic barcode for the São Francisco Craton: Contextual in-situ SHRIMP UPb baddeleyite and zircon dating of the Lavras, Pará de Minas and Formiga dyke swarms and implications for Columbia and Rodinia reconstructions. Lithos 374, 105708.

Cioffi, C.R., Campos Neto, M.C., Möller, A., Rocha, B.C., 2016a. Tectonic significance of the Meso-to Neoarchean complexes in the basement of the southern Brasília Orogen. Precambrian Res. 287, 91–107.

Cioffi, C.R., Campos Neto, M.C., Möller, A., Rocha, B.C., 2016b. Paleoproterozoic continental crust generation events at 2.15 and 2.08 Ga in the basement of the southern Brasília Orogen, SE Brazil. Precambrian Res. 275, 176–196.

Coelho, M.B., Trouw, R.A.J., Ganade, C.E., Vinagre, R., Mendes, J.C., Sato, K., 2017. Constraining timing and PT conditions of continental collision and late overprinting in the Southern Brasília Orogen (SE-Brazil): U-Pb zircon ages and geothermobarometry of the Andrelândia Nappe System. Precambrian Res. 292, 194–215.

Collins, W.J., Huang, H.Q., Bowden, P., Kemp, A.I.S., 2020. Repeated S-I–A-type granite trilogy in the Lachlan Orogen and geochemical contrasts with A-type granites in Nigeria: implications for petrogenesis and tectonic discrimination. Geol. Soc. London Spec. Pub. 491 (1), 53–76.

Condie, K.C., Aster, R.C., 2010. Episodic zircon age spectra of orogenic granitoids: the supercontinent connection and continental growth. Precambrian Res. 180 (3–4), 227–236.

Couzinié, S., Laurent, O., Moyen, J.F., Zeh, A., Bouilhol, P., Villaros, A., 2016. Post-collisional magmatism: crustal growth not identified by zircon Hf–O isotopes. Earth Planet. Sci. Lett. 456, 182–195.

Cutts, K., Lana, C., Alkmim, F., Farina, F., Moreira, H., Coelho, V., 2019. Metamorphism and exhumation of basement gneiss domes in the Quadrilátero Ferrífero: Two stage dome-and-keel evolution? Geosci. Front. 10 (5), 1765–1787.

Dall'Agnol, R., Teixeira, N.P., Rämö, O.T., Moura, C.A., Macambira, M.J., Oliveira, D.C., 2005. Petrogenesis of the Paleoproterozoic rapakivi A-type granites of the Archean Carajás metallogenic province, Brazil. Lithos 80 (1–4), 101–129.

Dall'Agnol, R., Oliveira, D.C., 2007. Oxidized, magnetite-series, rapakivi-type granites of Carajás, Brazil: implications for classification and petrogenesis of A-type granites. Lithos 93 (3–4), 215–233.

Davidson, J., Turner, S., Plank, T., 2013. Dy/Dy*: variations arising from mantle sources and petrogenetic processes. J. Petrol. 54 (3), 525–537.

Dhuime, B., Wuestefeld, A., Hawkesworth, C.J., 2015. Emergence of modern continental crust about 3 billion years ago. Nat. Geosci. 8 (7), 552.

Dopico, C.I.M., Lana, C., Moreira, H.S., Cassino, L.F., Alkmim, F.F., 2017. U-Pb ages and Hf-isotope data of detrital zircons from the late Neoarchean-Paleoproterozoic Minas Basin, SE Brazil. Precambrian Res. 291, 143–161.

Eby, G.N., 1992. Chemical subdivision of the A-type granitoids: petrogenetic and tectonic implications. Geology 20 (7), 641–644.

Farina, F., Albert, C., Lana, C., 2015. The Neoarchean transition between medium- and high-K granitoids: Clues from the Southern São Francisco Craton (Brazil). Precambrian Res. 266, 375–394.

Farina, F., Albert, C., Dopico, C.M., Gil, C.A., Moreira, H., Hippertt, J.P., Cutts, K., Alkmim, F.F., Lana, C., 2016. The Archean-Paleoproterozoic evolution of the Quadrilátero Ferrífero (Brasil): Current models and open questions. J. S. Am. Earth. Sci. 68, 4–21.

Fedele, L., Lustrino, M., Melluso, L., Morra, V., Zanetti, A., Vannucci, R., 2015. Trace-element partitioning between plagioclase, alkali feldspar, Ti-magnetite, biotite,

apatite, and evolved potassic liquids from Campi Flegrei (Southern Italy). Am. Miner. 100 (1), 233–249.
Foley, S., Tiepolo, M., Vannucci, R., 2002. Growth of early continental crust controlled by melting of amphibolite in subduction zones. Nature 417 (6891), 837–840.
Fontainha, M.V., Trouw, R.A.J., Dantas, E.L., Polo, H.J., Furtado, P.C., Marimon, R.S., Telles, R.C.M., Peternel, R., 2021. Provenance and tectonic evolution of the Andrelândia Group in the region between the Socorro and Guaxupé nappes, Southern Brasília and Ribeira orogens, Brazil. J. S. Am. Earth. Sci. 109, 103060.
Fowler, M., Rollinson, H., 2012. Phanerozoic sanukitoids from Caledonian Scotland: Implications for Archean subduction. Geology 40 (12), 1079–1082. https://doi.org/10.1130/G33371.1.
Frost, C.D., Frost, R.B., 1997. Reduced rapakivi-type granites: the tholeiite connection. Geology 25 (7), 647–650.
Frost, C.D., Frost, B.R., 2011. On ferroan (A-type) granitoids: their compositional variability and modes of origin. J. Petrol. 52 (1), 39–53.
Guo, Z., Wilson, M., 2012. The Himalayan leucogranites: constraints on the nature of their crustal source region and geodynamic setting. Gondwana Res. 22 (2), 360–376.
Halla, J., 2020. The TTG-amphibolite terrains of Arctic Fennoscandia: Infinite networks of amphibolite metatexite-diatexite transitions. Front. Earth Sci. 8, 252.
Hartmann, L.A., Endo, I., Suita, M.T.F., Santos, J.O.S., Frantz, J.C., Carneiro, M.A., McNaughton, N.J., Barley, M.E., 2006. Provenance and age delimitation of Quadrilátero Ferrífero sandstones based on zircon U-Pb isotopes. J. S. Am. Earth. Sci. 20 (4), 273–285.
Hawkesworth, C., Cawood, P., Dhuime, B., 2013. Continental growth and the crustal record. Tectonophysics 609, 651–660.
Hawkesworth, C., Cawood, P.A., Dhuime, B., 2020. The evolution of the continental crust and the onset of plate tectonics. Front. Earth Sci. 8, 326.
Hawkesworth, C., Kemp, T., 2021. A Pilbara perspective on the generation of Archaean continental crust. Chem. Geol. 578, 120326.
Heilimo, E., Halla, J., Hölttä, P., 2010. Discrimination and origin of the sanukitoid series: geochemical constraints from the Neoarchean western Karelian Province (Finland). Lithos 115 (1–4), 27–39.
Heilimo, E., Halla, J., Andersen, T., Huhma, H., 2013. Neoarchean crustal recycling and mantle metasomatism: Hf–Nd–Pb–O isotope evidence from sanukitoids of the Fennoscandian shield. Precambrian Res. 228, 250–266.
Hermann, J., 2002. Allanite: thorium and light rare earth element carrier in subducted crust. Chem. Geol. 192 (3–4), 289–306.
Hernández-Montenegro, J.D., Palin, R.M., Zuluaga, C.A., Hernández-Uribe, D., 2021. Archean continental crust formed by magma hybridization and voluminous partial melting. Sci. Rep. 11 (1), 1–9.
Hickman, A.H., 2012. Review of the Pilbara Craton and Fortescue Basin, Western Australia: crustal evolution providing environments for early life. Isl. Arc 21 (1), 1–31.
Holder, R.M., Viete, D.R., Brown, M., Johnson, T.E., 2019. Metamorphism and the evolution of plate tectonics. Nature 572 (7769), 378–381.
Jayananda, M., Chardon, D., Peucat, J.J., Capdevila, R., 2006. 2.61 Ga potassic granites and crustal reworking in the western Dharwar craton, southern India: tectonic, geochronologic and geochemical constraints. Precambrian Res. 150 (1–2), 1–26.
Jayananda, M., Aadhiseshan, K.R., Kusiak, M.A., Wilde, S.A., Sekhamo, K.U., Guitreau, M., Santosh, M., Gireesh, R.V., 2020. Multi-stage crustal growth and Neoarchean geodynamics in the Eastern Dharwar Craton, southern India. Gondwana Res. 78, 228–260.
Johnson, T.E., Brown, M., Gardiner, N.J., Kirkland, C.L., Smithies, R.H., 2017. Earth's first stable continents did not form by subduction. Nature 543 (7644), 239–242.
Kendrick, J., Duguet, M., Yakymchuk, C., 2022. Diversification of Archean tonalite-trondhjemite-granodiorite suites in a mushy middle crust. Geology 50 (1), 76–80.
Kusky, T., Windley, B.F., Polat, A., Wang, L., Ning, W., Zhong, Y., 2021. Archean dome-and-basin style structures form during growth and death of intraoceanic and continental margin arcs in accretionary orogens. Earth-Sci. Rev. 220, 103725.
Kuster, K., Ribeiro, A., Trouw, R.A.J., Dussin, I., Marimon, R.S., 2020. The Neoproterozoic Andrelândia group: Evolution from an intraplate continental margin to an early collisional basin south of the São francisco craton, Brazil. J. South Am. Earth Sci. 102, 102666.
Lana, C., Alkmim, F.F., Armstrong, R., Scholz, R., Romano, R., Nalini Jr, H.A., 2013. The ancestry and magmatic evolution of Archaean TTG rocks of the Quadrilátero Ferrífero province, southeast Brazil. Precambrian Res. 231, 157–173.
Laurent, O., Martin, H., Doucelance, R., Moyen, J.F., Paquette, J.L., 2011. Geochemistry and petrogenesis of high-K "sanukitoids" from the Bulai pluton, Central Limpopo Belt, South Africa: Implications for geodynamic changes at the Archaean-Proterozoic boundary. Lithos 123 (1–4), 73–91.
Laurent, O., Doucelance, R., Martin, H., Moyen, J.F., 2013. Differentiation of the late-Archaean sanukitoid series and some implications for crustal growth: insights from geochemical modelling on the Bulai pluton, Central Limpopo Belt, South Africa. Precambrian Res. 227, 186–203.
Laurent, O., Martin, H., Moyen, J.F., Doucelance, R., 2014a. The diversity and evolution of late-Archean granitoids: Evidence for the onset of "modern-style" plate tectonics between 3.0 and 2.5 Ga. Lithos 205, 208–235.
Laurent, O., Rapopo, M., Stevens, G., Moyen, J.F., Martin, H., Doucelance, R., Bosq, C., 2014b. Contrasting petrogenesis of Mg–K and Fe–K granitoids and implications for post-collisional magmatism: case study from the Late-Archean Matok pluton (Pietersburg block, South Africa). Lithos 196, 131–149.
Laurent, O., Zeh, A., 2015. A linear Hf isotope-age array despite different granitoid sources and complex Archean geodynamics: Example from the Pietersburg block (South Africa). Earth Planet. Sci. Lett. 430, 326–338.
Laurent, O., Zeh, A., Brandl, G., Vezinet, A., Wilson, A., 2019. Granitoids and greenstone belts of the Pietersburg block—Witnesses of an Archaean accretionary orogen along the northern edge of the Kaapvaal craton. The Archaean Geology of the Kaapvaal Craton, Southern Africa. Springer, Cham, pp. 83–107.
Laurent, O., Björnsen, J., Wotzlaw, J.F., Bretscher, S., Silva, M.P., Moyen, J.F., Ulmer, P., Bachmann, O., 2020. Earth's earliest granitoids are crystal-rich magma reservoirs tapped by silicic eruptions. Nat. Geosci. 13 (2), 163–169.
Laurie, A., Stevens, G., 2012. Water-present eclogite melting to produce Earth's early felsic crust. Chem. Geol. 314, 83–95.
Li, C., Arndt, N.T., Tang, Q., Ripley, E.M., 2015. Trace element indiscrimination diagrams. Lithos 232, 76–83.
Lobach-Zhuchenko, S.B., Rollinson, H., Chekulaev, V.P., Savatenkov, V.M., Kovalenko, A.V., Martin, H., Guseva, N.S., Arestova, N.A., 2008. Petrology of a Late Archaean, highly potassic, sanukitoid pluton from the Baltic Shield: insights into Late Archaean mantle metasomatism. J. Petrol. 49 (3), 393–420.
Lobato, L.M., Ribeiro-Rodrigues, L.C., Zucchetti, M., Noce, C.M., Baltazar, O.F., da Silva, L.C., Pinto, C.P., 2001. Brazil's premier gold province. Part I: The tectonic, magmatic, and structural setting of the Archean Rio das Velhas greenstone belt, Quadrilátero Ferrífero. Mineral. Deposita 36 (3–4), 228–248.
Ma, X., Guo, J., Liu, F., Qian, Q., Fan, H., 2013. Zircon U–Pb ages, trace elements and Nd–Hf isotopic geochemistry of Guyang sanukitoids and related rocks: Implications for the Archean crustal evolution of the Yinshan Block, North China Craton. Precambrian Res. 230, 61–78.
Machado, N., Noce, C.M., Ladeira, E.A., Oliveira, O.B., 1992. U-Pb geochronology of Archean magmatism and Proterozoic metamorphism in the Quadrilátero Ferrífero, southern São Francisco craton, Brazil. Geol. Soc. Am. Bull. 104 (9), 1221–1227.
Marangoanha, B., Oliveira, D.C., Oliveira, V.E.S., Galarza, M.A., Lamarão, C.N., 2019. Neoarchean A-type granitoids from Carajás province (Brazil): New insights from geochemistry, geochronology and microstructural analysis. Precambrian Res. 324, 86–108.
Marimon, R.S., Trouw, R.A.J., Dantas, E.L., Ribeiro, A., 2020a. U-Pb and Lu-Hf isotope systematics on detrital zircon from the southern São Francisco Craton's Neoproterozoic passive margin: Tectonic implications. J. S. Am. Earth. Sci. 100, 102539.
Marimon, R.S., Trouw, R.A.J., Dantas, E.L., 2020b. Significance of age periodicity in the continental crust record: The São Francisco Craton and adjacent Neoproterozoic orogens as a case study. Gondwana Res. 86, 144–163.
Marimon, R.S., Trouw, R.A.J., Dantas, E.L., Ribeiro, A., Santos, P., Kuster, K., Vinagre, R., 2021. Provenance of passive-margin and syn-collisional units: Implications for the geodynamic evolution of the Southern Brasília Orogen, West Gondwana. Sediment. Geol. 413, 105823.
Martin, H., 1986. Effect of steeper Archean geothermal gradient on geochemistry of subduction-zone magmas. Geology 14 (9), 753–756.
Martin, H., 1987. Petrogenesis of Archaean trondhjemites, tonalites, and granodiorites from eastern Finland: major and trace element geochemistry. J. Petrol. 28 (5), 921–953.
Martin, H., Moyen, J.F., Rapp, R., 2009. The sanukitoid series: magmatism at the Archaean-Proterozoic transition. Earth Environ. Sci. Trans. Res. Soc. 100 (1–2), 15–33.
Martin, H., Moyen, J.F., Guitreau, M., Blichert-Toft, J., Le Pennec, J.L., 2014. Why Archaean TTG cannot be generated by MORB melting in subduction zones. Lithos 198, 1–13.
McDonough, W.F., Sun, S.S., 1995. The composition of the Earth. Chem. Geol. 120 (3–4), 223–253.
Melo-Silva, P., Amaral, W.S., Oliveira, E.P., 2020. Geochronological evolution of the Pitangui greenstone belt, southern São Francisco craton, Brazil: Constraints from U-Pb zircon age, geochemistry and field relationships. J. S. Am. Earth. Sci. 99, 102380.
Mikkola, P., Lauri, L.S., Käpyaho, A., 2012. Neoarchean leucogranitoids of the Kianta Complex, Karelian Province, Finland: source characteristics and processes responsible for the observed heterogeneity. Precambrian Res. 206, 72–86.
Moreno, J.A., Baldim, M.R., Semprich, J., Oliveira, E.P., Verma, S.K., Teixeira, W., 2017. Geochronological and geochemical evidences for extension-related Neoarchean granitoids in the southern São Francisco Craton, Brazil. Precambrian Res. 294, 322–343.
Moreira, H., Lana, C., Nalini Jr, H.A., 2016. The detrital zircon record of an Archaean convergent basin in the Southern São Francisco Craton, Brazil. Precambrian Res. 275, 84–99.
Moreira, H., Cassino, L., Lana, C., Storey, C., Albert, C., 2019. Insights into orogenic processes from drab schists and minor intrusions: Southern São Francisco Craton, Brazil. Lithos 346, 105146.
Moyen, J.F., 2011. The composite Archaean grey gneisses: petrological significance, and evidence for a non-unique tectonic setting for Archaean crustal growth. Lithos 123 (1–4), 21–36.
Moyen, J.F., Martin, H., 2012. Forty years of TTG research. Lithos 148, 312–336.
Moyen, J.F., Laurent, O., 2018. Archaean tectonic systems: a view from igneous rocks. Lithos 302, 99–125.
Moyen, J.F., Zeh, A., Cuney, M., Dziggel, A., Carrouée, S., 2021. The multiple ways of recycling Archaean crust: a case study from the ca. 3.1 Ga granitoids from the Barberton Greenstone Belt, South Africa. Precambrian Res. 353, 105998.

Noce, C.M., Machado, N., Teixeira, W., 1998. U-Pb geochronology of gneisses and granitoids in the Quadrilatero Ferrifero (Southern Sao Francisco craton, Brazil): age constraints for Archean and Paleoproterozoic magmatism and metamorphism. Revista Brasileira de Geociências 28 (1), 95–102.
Noce, C.M., 2000. Geochronology of the Quadrilátero Ferrífero: a review. Geonomos 8 (1), 15–23.
Noce, C.M., Zuccheti, M., Baltazar, O.F., Armstrong, R., Dantas, E., Renger, F.E., Lobato, L.M., 2005. Age of felsic volcanism and the role of ancient continental crust in the evolution of the Neoarchean Rio das Velhas Greenstone belt (Quadrilátero Ferrífero, Brazil): U-Pb zircon dating of volcaniclastic graywackes. Precambrian Res. 141 (1–2), 67–82.
Noce, C.M., Pedrosa-Soares, A.C., Silva, L.C., Armstrong, R., Piuzana, D., 2007. Evolution of polycyclic basement complexes in the Araçuaí Orogen, based on U-Pb SHRIMP data: Implications for Brazil-Africa links in Paleoproterozoic time. Precambrian Res. 159 (1–2), 60–78.
O'Connor, J.T., 1965. A classification for quartz-rich igneous rocks. Geological Survey Professional Paper 525, 79.
Oliveira, M.A.F., Negri, F.A., Zanardo, A., Morales, N., 2019. Archean and paleoproterozoic crust generation events, Amparo complex and Serra Negra orthogneiss in southern Brasília Orogen, SE Brazil. J. S. Am. Earth. Sci. 90, 137–154.
Palin, R.M., White, R.W., Green, E.C., 2016. Partial melting of metabasic rocks and the generation of tonalitic–trondhjemitic–granodioritic (TTG) crust in the Archaean: Constraints from phase equilibrium modelling. Precambrian Res. 287, 73–90.
Patiño Douce, A.E., Beard, J.S., 1995. Dehydration-melting of biotite gneiss and quartz amphibolite from 3 to 15 kbar. J. Petrol. 36 (3), 707–738.
Patiño Douce, A.E., 1997. Generation of metaluminous A-type granites by low-pressure melting of calc-alkaline granitoids. Geology 25 (8), 743–746.
Patiño Douce, A.E., McCarthy, T.C., 1998. Melting of crustal rocks during continental collision and subduction. In: When Continents Collide: Geodynamics and Geochemistry of Ultrahigh-Pressure Rocks. Springer, Dordrecht, pp. 27–55.
Patiño Douce, A.E., 2005. Vapor-absent melting of tonalite at 15–32 kbar. J. Petrol. 46 (2), 275–290.
Pearce, J.A., 2008. Geochemical fingerprinting of oceanic basalts with applications to ophiolite classification and the search for Archean oceanic crust. Lithos 100. https://doi.org/10.1016/j.lithos.2007.06.016.
Pourteau, A., Doucet, L.S., Blereau, E.R., Volante, S., Johnson, T.E., Collins, W.J., Li, Z.X., Champion, D.C., 2020. TTG generation by fluid-fluxed crustal melting: Direct evidence from the Proterozoic Georgetown Inlier, NE Australia. Earth Planet. Sci. Lett. 550, 116548.
Rapp, R.P., Watson, E.B., Miller, C.F., 1991. Partial melting of amphibolite/eclogite and the origin of Archean trondhjemites and tonalites. Precambrian Res. 51 (1–4), 1–25.
Rapp, R.P., Watson, E.B., 1995. Dehydration melting of metabasalt at 8–32 kbar: implications for continental growth and crust-mantle recycling. J. Petrol. 36 (4), 891–931.
Rapp, R.P., Shimizu, N., Norman, M.D., Applegate, G.S., 1999. Reaction between slab-derived melts and peridotite in the mantle wedge: experimental constraints at 3.8 GPa. Chem. Geol. 160 (4), 335–356.
Rapp, R.P., Shimizu, N., Norman, M.D., 2003. Growth of early continental crust by partial melting of eclogite. Nature 425 (6958), 605–609.
Romano, R., Lana, C., Alkmim, F.F., Stevens, G., Armstrong, R., 2013. Stabilization of the southern portion of the São Francisco craton, SE Brazil, through a long-lived period of potassic magmatism. Precambrian Res. 224, 143–159.
Santos, C.A., 2014. Geologia, petrografia e geocronologia dos gnaisses e rochas associadas na região entre Carrancas, Minduri e Luminárias (MG). University of São Paulo (in Portuguese). M.S. thesis.
Sardinha, A.S., Barros, C.E.M., Krymsky, R., 2006. Geology, geochemistry, and U-Pb geochronology of the Archean (2.74 Ga) Serra do Rabo granite stocks, Carajás Metallogenetic Province, northern Brazil. J. S. Am. Earth. Sci. 20 (4), 327–339.
Savko, K.A., Samsonov, A.V., Kholina, N.V., Larionov, A.N., Zaitseva, M.V., Korish, E.H., Bazikov, N.S., Terentiev, R.A., 2019. 2.6 Ga high-Si rhyolites and granites in the Kursk Domain, Eastern Sarmatia: Petrology and application for the Archaean palaeocontinental correlations. Precambrian Res. 322, 170–192.
Sawyer, E.W., Cesare, B., Brown, M., 2011. When the continental crust melts. Elements 7 (4), 229–234.
Sen, C., Dunn, T., 1994. Dehydration melting of a basaltic composition amphibolite at 1.5 and 2.0 GPa: implications for the origin of adakites. Contrib. Mineral. Petrol. 117 (4), 394–409.
Shirey, S.B., Hanson, G.N., 1984. Mantle-derived Archaean monozodiorites and trachyandesites. Nature 310 (5974), 222–224.
Simon, M.B., Bongiolo, E.M., Avila, C.A., Oliveira, E.P., Teixeira, W., Stohler, R.C., Oliveira, F.V.S., 2018. Neoarchean reworking of TTG-like crust in the southernmost portion of the São Francisco Craton: U-Pb zircon dating and geochemical evidence from the São Tiago Batholith. Precambrian Res. 314, 353–376.
Simon, M.B., Bongiolo, E.M., Ávila, C.A., Teixeira, W., Marimon, R.S., Oliveira, E.P., 2021. Archean sodic metagranitoids from the Southern São Francisco Craton: Review, petrogenesis, and tectonic implications. Lithos 106246.
Sisson, T.W., Ratajeski, K., Hankins, W.B., Glazner, A.F., 2005. Voluminous granitic magmas from common basaltic sources. Contrib. Mineral. Petrol. 148 (6), 635–661.
Skjerlie, K.P., Johnston, A.D., 1992. Vapor-absent melting at 10 kbar of a biotite-and amphibole-bearing tonalitic gneiss: implications for the generation of A-type granites. Geology 20 (3), 263–266.
Skjerlie, K.P., Johnston, A.D., 1993. Fluid-absent melting behavior of an F-rich tonalitic gneiss at mid-crustal pressures: implications for the generation of anorogenic granites. J. Petrol. 34 (4), 785–815.
Smit, M.A., Mezger, K., 2017. Earth's early O_2 cycle suppressed by primitive continents. Nat. Geosci. 10 (10), 788–792.
Smithies, R.H., 2000. The Archaean tonalite–trondhjemite–granodiorite (TTG) series is not an analogue of Cenozoic adakite. Earth Planet. Sci. Lett. 182 (1), 115–125.
Smithies, R.H., Champion, D.C., Van Kranendonk, M.J., 2009. Formation of Paleoarchean continental crust through infracrustal melting of enriched basalt. Earth Planet. Sci. Lett. 281 (3–4), 298–306.
Brando-Soares, M., Corrêa Neto, A.V., Zeh, A., Cabral, A.R., Pereira, L.F., Prado, M.G.B., Almeida, A.M., Manduca, L.G., Silva, P.H.M., Mabub, R.O.A., Schlichta, T.M., 2017. Geology of the Pitangui greenstone belt, Minas Gerais, Brazil: stratigraphy, geochronology and BIF geochemistry. Precambrian Res. 291, 17–41.
Brando-Soares, M., Corrêa Neto, A.V., Fabricio-Silva, W., 2020. The development of a Meso-to Neoarchean rifting-convergence-collision-collapse cycle over an ancient thickened protocontinent in the south São Francisco craton, Brazil. Gondwana Res. 77, 40–66.
Springer, W., Seck, H.A., 1997. Partial fusion of basic granulites at 5 to 15 kbar: implications for the origin of TTG magmas. Contrib. Mineral. Petrol. 127 (1–2), 30–45.
Teixeira, W., Carneiro, M.A., Noce, C.M., Machado, N., Sato, K., Taylor, P.N., 1996. Pb, Sr and Nd isotope constraints on the Archaean evolution of gneissic-granitoid complexes in the southern São Francisco Craton, Brazil. Precambrian Res. 78 (1–3), 151–164.
Teixeira, W., Cordani, U.G., Nutman, A.P., Sato, K., 1998. Polyphase Archean evolution in the Campo Belo metamorphic complex, Southern São Francisco Craton, Brazil: SHRIMP U-Pb zircon evidence. J. S. Am. Earth. Sci. 11 (3), 279–289.
Teixeira, W., Ávila, C.A., Dussin, I.A., Neto, A.C., Bongiolo, E.M., Santos, J.O., Barbosa, N.S., 2015. A juvenile accretion episode (2.35–2.32 Ga) in the Mineiro belt and its role to the Minas accretionary orogeny: Zircon U-Pb–Hf and geochemical evidences. Precambrian Res. 256, 148–169.
Teixeira, W., Oliveira, E.P., Marques, L.S., 2017. Nature and evolution of the Archean crust of the São Francisco Craton. In: Heilbron, M., Cordani, U., Alkmim, F. (Eds.), São Francisco Craton, Eastern Brazil. Regional Geology Reviews. Springer, Cham, pp. 29–56. https://doi.org/10.1007/978-3-319-01715-0_3.
Trouw, R.A., Peternel, R., Ribeiro, A., Heilbron, M., Vinagre, R., Duffles, P., Trouw, C.C., Fontainha, M., Kussama, H.H., 2013. A new interpretation for the interference zone between the southern Brasília belt and the central Ribeira belt, SE Brazil. J. S. Am. Earth. Sci. 48, 43–57.
Valeriano, C.M., Pimentel, M.M., Heilbron, M., Almeida, J.C.H., Trouw, R.A.J., 2008. Tectonic evolution of the Brasília Belt, Central Brazil, and early assembly of Gondwana. Geol. Soc. London Spec. Pub. 294 (1), 197–210.
Valeriano, C.M., Turbay, C.V.G., Bruno, H., Simonetti, A., Heilbron, M., Bersan, S.M., Strachan, R., 2022. Paleo- and Mesoarchean TTG-sanukitoid to high-K granite cycles in the southern São Francisco craton, SE Brazil. Geosci. Front., 101372
Vander Auwera, J., Bogaerts, M., Liégeois, J.P., Demaiffe, D., Wilmart, E., Bolle, O., Duchesne, J.C., 2003. Derivation of the 1.0–0.9 Ga ferro-potassic A-type granitoids of southern Norway by extreme differentiation from basic magmas. Precambrian Res. 124 (2–4), 107–148.
Verma, S.K., Oliveira, E.P., Silva, P.M., Moreno, J.A., Amaral, W.S., 2017. Geochemistry of komatiites and basalts from the Rio das Velhas and Pitangui greenstone belts, São Francisco Craton, Brazil: Implications for the origin, evolution, and tectonic setting. Lithos 284, 560–577.
Vinagre, R., Trouw, R.A.J., Marimon, R.S., Nepomuceno, F., Mendes, J.C., Dantas, E.L., 2020. São Bento do Sapucaí Shear Zone: Constraining age and P-T conditions of a collisional Neoproterozoic oblique shear zone, Ribeira Orogen, Brazil. J. South Am. Earth Sci. 98, 102418.
Vinagre, R., Trouw, R.A., Mendes, J.C., Duffles, P., Peternel, R., Matos, G., 2014. New Evidence of a Magmatic Arc in the Southern Brasília Belt, Brazil: The Serra da Água Limpa Batholith (Socorro-Guaxupé Nappe). J. S. Am. Earth. Sci. 54, 120–139.
Watkins, J.M., Clemens, J.D., Treloar, P.J., 2007. Archaean TTGs as sources of younger granitic magmas: melting of sodic metatonalites at 0.6–1.2 GPa. Contrib. Mineral. Petrol. 154 (1), 91–110.
Windley, B.F., Kusky, T., Polat, A., 2021. Onset of plate tectonics by the Eoarchean. Precambrian Res. 352, 105980.
Winther, K.T., 1996. An experimentally based model for the origin of tonalitic and trondhjemitic melts. Chem. Geol. 127 (1–3), 43–59.
Wolf, M.B., Wyllie, P.J., 1994. Dehydration-melting of amphibolite at 10 kbar: the effects of temperature and time. Contrib. Mineral. Petrol. 115 (4), 369–383.
Ye, Z., Wan, F., Jiang, N., Xu, J., Wen, Y., Fan, D., Zhou, W., 2021. Dehydration melting of amphibolite at 1.5 GPa and 800–950 °C: Implications for the Mesozoic potassium-rich adakite in the eastern North China Craton. Geosci. Front. 12 (2), 896–906.
Zeh, A., Jaguin, J., Poujol, M., Boulvais, P., Block, S., Paquette, J.L., 2013. Juvenile crust formation in the northeastern Kaapvaal Craton at 2.97 Ga—Implications for Archean terrane accretion, and the source of the Pietersburg gold. Precambrian Res. 233, 20–43.
Zhou, G., Wu, Y., Gao, S., Yang, J., Zheng, J., Qin, Z., Wang, H., Yang, S., 2015. The 2.65 Ga A-type granite in the northeastern Yangtze craton: Petrogenesis and geological implications. Precambrian Res. 258, 247–259.
Zucchetti, M., Lobato, L.M., Baars, F.J., 2000. Genetically diverse basalt geochemical signatures developed in the Rio das Velhas greenstone belt, Quadrilátero Ferrífero, Minas Gerais, Brazil. Revista Brasileira de Geociências 30 (3), 397–402.